FUTURE ENERGY

SPECIAL ISSUE   Volume 4 No. 2 $5
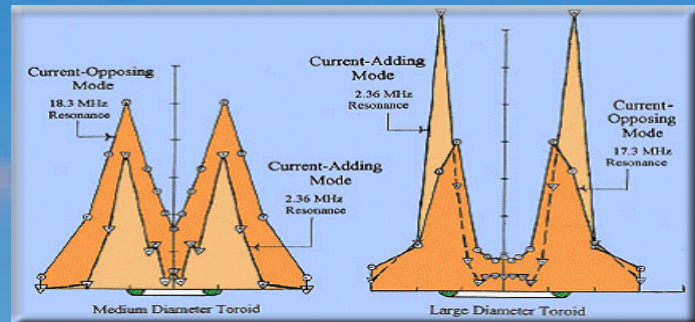
COFE

Fourth International Conference

March 15-17, 2011

Steep magnetic field gradients forming in the radial direction over tightly-wound toroidal coils with no magnetic field on the inside of the coils which are in the current-opposing mode. Tested at Froning Labs.

Atomic Force Microscope testing the dynamics of the ferro magnets in the Coler apparatus at the Ludwig Labs. Device investigated also by British Intelligence in 1947.

ENERGY
PROPULSION
BIOENERGETICS

iRi

www.IntegrityResearchInstitute.org

Space, Propulsion & Energy Sciences International Forum

March 15-17, 2011

University of Maryland, College Park, MD

http://www.ias-spes.org/SPESIF.html

SPESIF

IS an international technical forum organized by the **Institute for Advanced Studies in the Space, Propulsion & Energy Sciences (IASSPES)**.

The SPESIF platform seeks to promote the exchange of information among technologists, academicians, industrialists, and program managers on technical and programmatic issues related to the Space, Propulsion and Energy Sciences.
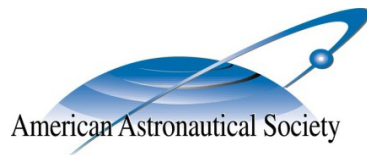
Among its organizers, conference and session chairs, and attendees, are high-level representatives from industry, government agencies, and institutes of higher learning.

Papers approved for SPESIF are reviewed by the technical staff, Chairs and Co-Chairs and other Committee Members needed for a proper peer review.

Organizing Chair: **Glen A. Robertson**, 265 Ita Ann Ln., Madison, AL 35757, 256-694-7941

SPESIF-2011 is organized In Co-Operation with

Future Energy

Special Conference Edition
COFE4 Summer 2011

Table of Contents

Editor's Note

We are pleased to bring to you a selection of future energy papers from the most vital and futuristic conference in the world, SPESIF-COFE, held at the University of Maryland, March 15-17, 2011 under the auspices of the UMD-SPPL and Professor Raymond Sedwick.

It is a further advancement of the legacy of Dave Froning to contribute his toroidal coil experiments, showing anomalous magnetic field gradients outside of the contra-wound coils having no magnetic field inside. The theory of scalar fields and vector potentials certainly comes into play in this work. Readers of *Future Energy* will recall Prof. Froning's paper and slideshow from COFE3 which dramatically showed the application of such energized toroidal coils in the alterations of the permeability and permittivity of the vacuum of space, theoretically enabling a propulsive force that enhances movement of the craft. Whenever I refer to Froning's work in my presentations, it is interesting to note that the effect he has discovered is enhanced at temperatures approaching absolute zero (outer space sits at about 3°K absolute). We hope to see scale model demonstrations soon!

After years of selling the historical report, "The Invention of Hans Coler, An Alleged New Power Source" authored by R. Hurst of the British Intelligence Objectives Subcommittee from 1947, it is a pleasure to see Dr. Ludwig's well-designed reproduction of the Coler device tested in his laboratory. Credit is due to Andreas Manthey for organizing the construction of the circuit. This is how science should progress…with unbiased evaluations of energy devices that are judged worthy of further test and investigation.

Moray King's article on water electrolyzers serves as an excellent review article for all those investigating claims of excess energy production. Following this with the interesting "Flow of Energy" article by Znidarsic and Robertson seems appropriate for a wider understanding of electron flow and nuclear mechanical waves that can appear in physics.

Osamu Ide's article on several anomalous results from his second-order magnetic gradients, called a "positive EMF" is fascinating and worthy of the reader's attention. It is also very significant that there was a temperature reduction in the magnetic cores, which is reminiscent of the Russian Godin and Roshchin experiments, now replicated by Paul Murad (see oral presentation at SPESIF-COFE 2011). Paul reports that he will submit a full paper by next conference time. Ide's 1995 applied physics article on a similar circuit effect is also reproduced for the reader's benefit.

Lastly, it is worthwhile to focus on a life extension discovery by graduate student Scott Kelsey, with advisor Dr. Norm Shealy, which has proven to lengthen the DNA ends called telomeres with an electromagnetic resonance exposure, that also is demonstrated in the conference exhibit hall.

Thomas Valone, PhD, PE

Integrity Research Institute
5020 Sunnyside Avenue, Suite 209
Beltsville Maryland 20705
301-220-0440, 888-802-5243
www.IntegrityResearchInstitute.org

Electromagnetic Radiation Experiments with Transmitting, Contra-Wound Toroidal Coils

H. David Froning,[a] George D. Hathaway[b] and Blair Cleveland[b]

[a] PO Box1211
Malibu CA, 90262, USA
310-459-5291; froning@infomagic.net

[b]Hathaway Consulting Services
1080 19th Sideroad
King City, L7B1KS, Ontario, Canada
ghathaway@ieee.org

Abstract. Except for Quantum Electrodynamics, there has been no real extension of Maxwell's classical electromagnetic (EM) field theory since his electromagnetic EM field equations were developed in 1864. These equations describe the behavior of vector fields of low (U1) Lie group symmetry. In this respect, Terence W. Barrett has used topology, group and gauge theory, to extend Maxwell theory into tensor fields of higher symmetry form: SU (2), SU (3), and higher, that describe the behavior of specially conditioned EM fields. One of Barrett's ways of emitting SU(2) EM fields was driving alternating current through toroidal coils at any of the resonant frequencies that will occur for a specific toroid geometry. Experiments to explore the possibility of achieving such resonant frequencies and SU(2) EM emissions will be described.

INTRODUCTION

In 1864 Maxwell described a unification of electricity and magnetism with equations that later followers distilled into the four equations now known as the "Maxwell equations" that conform to the laws of electromagnetism (EM) formulated by Gauss, Ampere, Coulomb and Faraday. In the 1950's Feynman and others made Maxwell's classical EM theory compatible with Quantum theory and resulted in Quantum Electrodynamics (QED). QED was consistent with both quantum mechanics and special relativity and precisely predicted interactions between radiation and matter. But, despite its reformulation from quaternionic to vector algebra form, no extension of Maxwell theory has been made during its 146 years of life - despite the inability to accurately explain many observed EM phenomena.

In most cases, EM radiation fields are correctly and adequately described by the classical Maxwell equations which is a theory of U(1) symmetry form. However, in special topologies or situations or boundary conditions, radiation fields are produced that require an extension of Maxwell theory to higher symmetry. Addressing such situations, Barrett (2008) has used topology, group and gauge to derive SU(2) EM radiation fields for those cases of specially conditioned radiation. A specific SU(2) EM radiation field proposed by Barrett is that which is emitted by toroidal coils when alternating current flows through them at any of the resonant frequencies that will occur for a specific toroid geometry. Toroidal coils have been constructed and tested, and. this paper summarizes testing results.

MAXWELL EQUATIONS FOR ORDINARY AND CONDITIONED EM FIELDS

Using group theoretic methods, EM radiation fields of SU(2) symmetry can be created by special conditioning of conventional U(1) EM fields. Table 1 shows Maxwell's (U(1) symmetry) four equations describing electric field strength (**E**), magnetic flux density (**B**) and current density (**J**). The **E** and **B** fields of force can be related to a "magnetic vector potential" (**A**) and "scalar electric potential" (*φ*). These potentials are unphysical and mere mathematical conveniences in terms of the U(1) field theory. However, in the SU(2) field theory, the potentials **A** and *φ* do have physicality (Barrett, 2008). Table 2 shows extended Maxwell equations that describe propagation of specially conditioned SU(2) EM fields. These Maxwell Equations are based on tensor, rather than vector field terms, and include **E** and **B** fields as U(1) Maxwell Equations do. But they include additional terms: (i) which can be viewed as the square root of -1 or as an orthogonal rotation occurring in x, y, z, ct spacetime; electron charge (*q*); and added interactions *A x E, A x B, A • E*; and *A• B* (Barrett, 2008, pp 145-147). These tensors, or matrices function as operators obeying non-commutative, non-Abelian algebra. So, *A x B* does not = *B x A* for SU(2) fields.

TABLE 1. Maxwell Equations for Ordinary U(1) EM Fields.

Gauss' Law	$\nabla \bullet \boldsymbol{E} = \boldsymbol{J}_0$
Ampere's Law	$\dfrac{\partial \boldsymbol{E}}{\partial t} - \nabla \times \boldsymbol{B} - \boldsymbol{J} = 0$
Coulomb's Law	$\nabla \bullet \boldsymbol{B} = 0$
Faraday's Law	$\nabla \times \boldsymbol{E} + \dfrac{\partial \boldsymbol{B}}{\partial t} = 0$

$$E = -\frac{\partial A}{\partial t} - \nabla\phi, \quad B = \nabla \times A$$

TABLE 2. Maxwell Equations for Specially Conditioned SU(2) tensor EM Fields (Barrett 2008).

$\nabla \bullet \boldsymbol{E} = \boldsymbol{J}_0 - iq(\boldsymbol{A} \bullet \boldsymbol{E} - \boldsymbol{E} \bullet \boldsymbol{A})$
$\dfrac{\partial \boldsymbol{E}}{\partial t} - \nabla \times \boldsymbol{B} - \boldsymbol{J} + iq[\boldsymbol{A}_0, \boldsymbol{E}] - iq(\boldsymbol{A} \times \boldsymbol{B} - \boldsymbol{B} \times \boldsymbol{A}) = 0$
$\nabla \bullet \boldsymbol{B} + iq(\boldsymbol{A} \bullet \boldsymbol{B} - \boldsymbol{B} \bullet \boldsymbol{A}) = 0$
$\nabla \times \boldsymbol{E} + \dfrac{\partial \boldsymbol{B}}{\partial t} + iq[\boldsymbol{A}_0, \boldsymbol{B}] = iq(\boldsymbol{A} \times \boldsymbol{E} - \boldsymbol{E} \times \boldsymbol{A}) = 0$

Noting that, unlike fields of Table 1, these fields are tensor (matrix operator) fields not vector fields**.**

The well known Lorentz force (**F**) arises from an electromagnetic interaction that involves **B** and **E** fields and the velocity (**v**) of charge clusters with charge (e). Table 3 shows force equations for both the U(1) EM vector fields in terms of the magnetic vector potentials and electric scalar potentials that underlie these U(1) vector fields and SU(2) tensor fields in terms of the vector and scalar potentials and it is noted that extra terms are in the SU(2) force equation. Thus, SU(2) field interaction forces can be different in magnitude and direction than U(1) field forces.

TABLE 3. Lorentz Force comparison for U(1) EM and SU(2) EM Fields (Barrett, 2008).

| U(1) Lorentz Force	$\mathscr{F} = e\mathbf{E} + ev \times \mathbf{B} = e\left(-\frac{\partial \mathbf{A}}{\partial t} - \nabla\phi \right)$ $+ ev \times \left((\nabla \times \mathbf{A}) \right)$
SU(2) Lorentz Force	$\mathscr{F} = e\mathbf{E} + ev \times \mathbf{B} = e\left(-(\nabla \times \mathbf{A}) - \frac{\partial \mathbf{A}}{\partial t} - \nabla\phi \right)$ $+ ev \times \left((\nabla \times \mathbf{A}) - \frac{\partial \mathbf{A}}{\partial t} - \nabla\phi \right)$

SU(2) EM RADIATION FROM TOROIDAL COILS AT RESONANT FREQUENCIES

Barrett (1998) describes one way of emitting SU(2) EM radiation. It is driving alternating current through toroidal coils at any of the resonant frequencies that will occur for the specific toroid geometry. Figure 1 shows the EM field pattern of a transmitting toroid as a U(1) A potential field overlapping in polarity across the toroid – with a set of equipotential lines of φ_1 pattern and another set of equipotential lines of φ_2 pattern. Also shown is a resonant frequency when the phase is such that (φ_1- φ_2) is maximal, and the various resonant radio frequencies that can occur for a given toroid. At every resonant frequency, the alternating difference in the U(1) potential fields is maximized for the whole toroid. An SU(2) potential field is maximized as well and this results in a maximum transmitted signal.
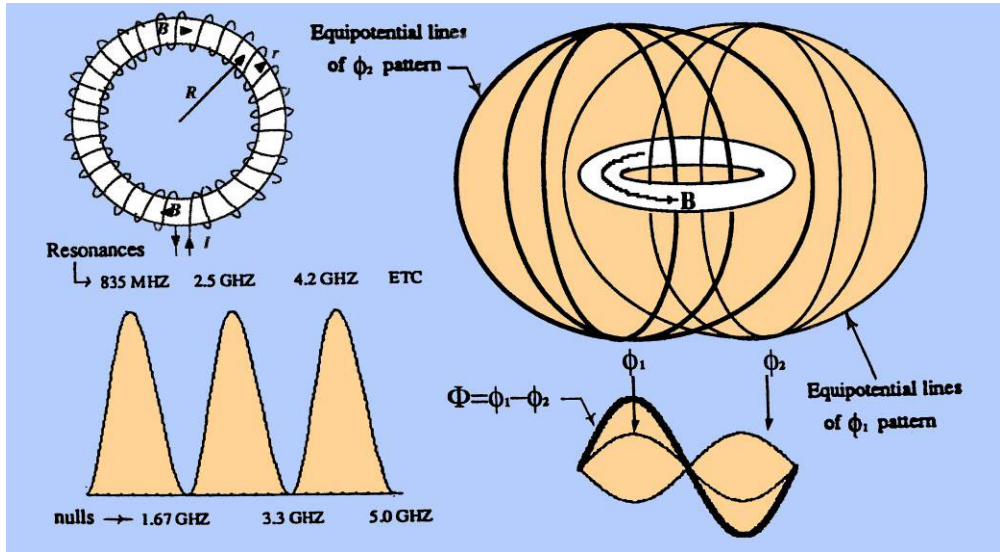
Figure 1. Potential patterns surrounding transmitting toroidal coils.

It was expected that resonant frequencies for radiating toroids would be revealed at the frequencies where the phase of alternating current would reverse and feed-point impedance would peak. Toroidal coils configured to emit SU(2) EM radiation were tested at Hathaway Consulting Services. Frequency sweeps revealed resonances for every tested toroid. Figure 2 shows good agreement between measured resonant frequencies and resonant frequencies predicted by Barrett (1998; 2000) for SU(2) field emission. The sweeps also revealed that EM fields emitted from each toroid would dramatically increase in strength within those narrow frequency bands where the resonances occurred.
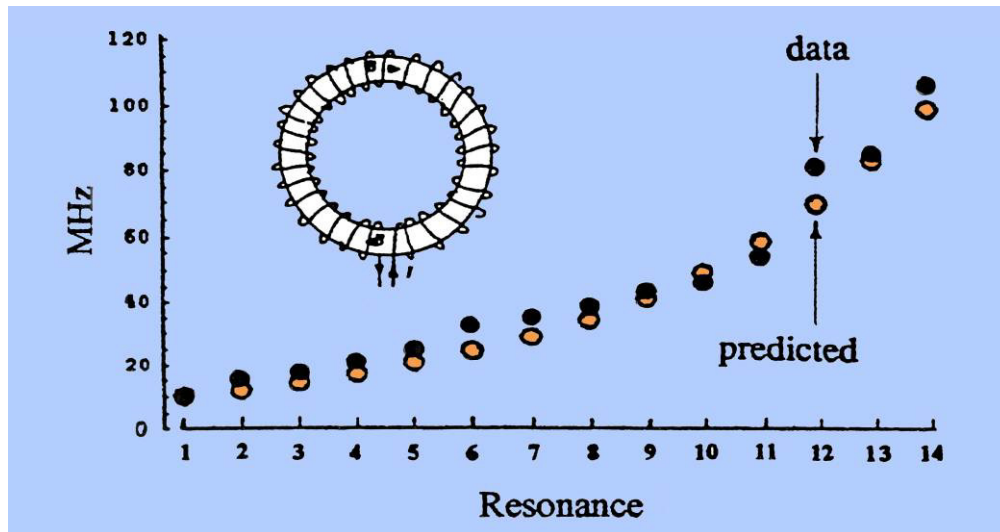
Figure 2. Good agreement between predicted and measured resonant frequencies.

The encouraging initial observations resulted in testing of 4 different toroid configurations shown in Figure 3. They typified variations in toroid major and minor diameter and coil winding density; and included asymmetric shapes. All toroids embodied contra-wound (caduceus) coils whose two interwoven wires make the same pattern as DNA strands. This allowed a current-adding mode, where equal currents flow in the 2 wires in the same direction through the coil; and a current-opposing mode, where equal current flowed in each wire in opposite directions. And, magnetic field probes confirmed that no magnetic field was induced inside each coil for this current-opposing mode.
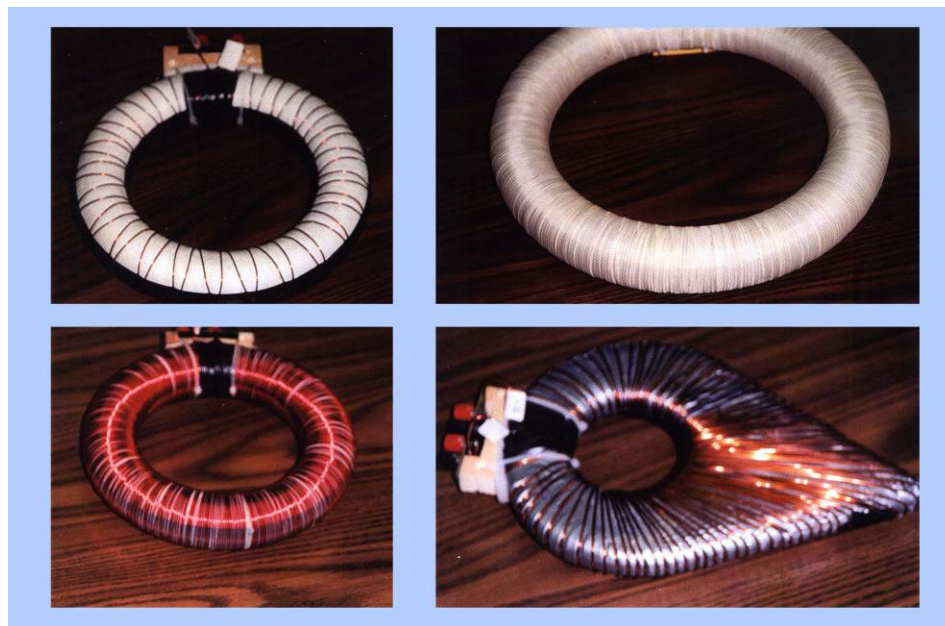
Figure 3. Various contra-wound caduceus toroids that were tested in second test series**.**

Radio-Frequency sweeping with equipment such as that shown in Figure 4 was conducted to find all resonant frequencies existing in the 400 KHz to 110 MHz range for each toroid. This was done for both current-adding and opposing modes of operation. Then, for at least one resonant frequency for each toroid, magnetic field strength was measured on the surface of (and, in the vicinity of,) each toroid for the current-adding and current-opposing modes.

Figure 4. Typical equipment (HP impedance analyzer and plotter) for detecting resonant toroid frequencies.

Figure 5 shows the response of the larger diameter toroid to flowing alternating current in it at frequencies from 400 KHz to 110 MHz for current-adding and current-opposing modes. Shown are many resonances occurring over the frequency spectrum in current-adding mode. Fewer (but much stronger) resonances occur in current-opposing mode,
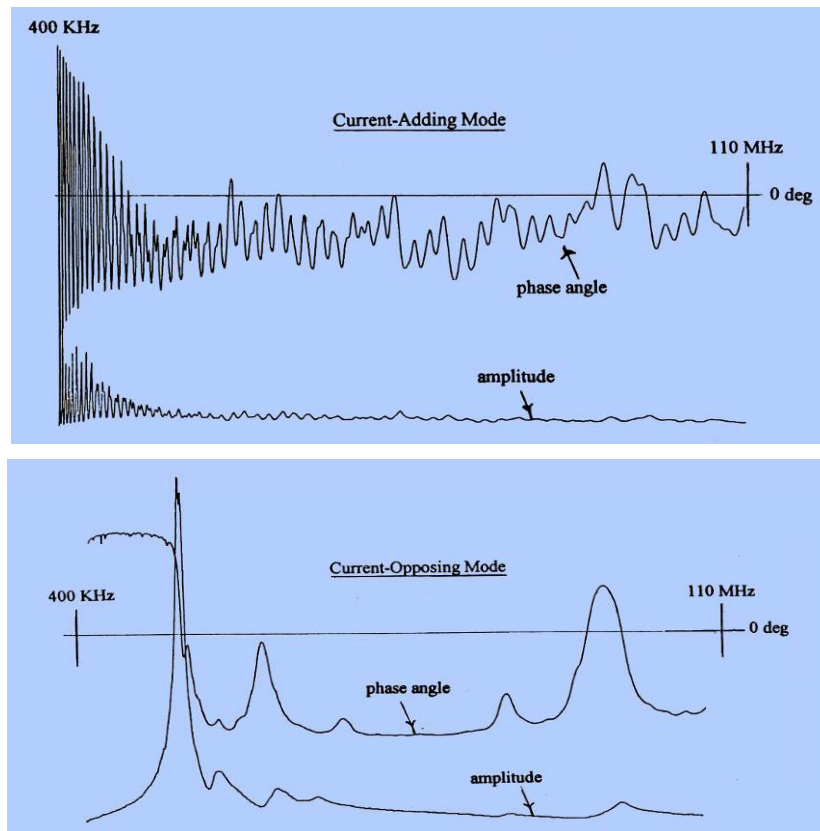
Figure 5. Larger diameter toroid response to frequency in current-adding and current-opposing modes.

Figure 6 shows the magnetic probe used to measure the vertical component of magnetic field intensity at locations on and near the surface of each toroid when the toroid was radiating at resonant frequency. It must be noted that this magnetic probe could not detect the individual undulations of any SU(2) A fields emitted by the toroids. But probe presence would cause symmetry breaking of any SU(2) A fields into U(1) B fields that the U(1) probe could detect.
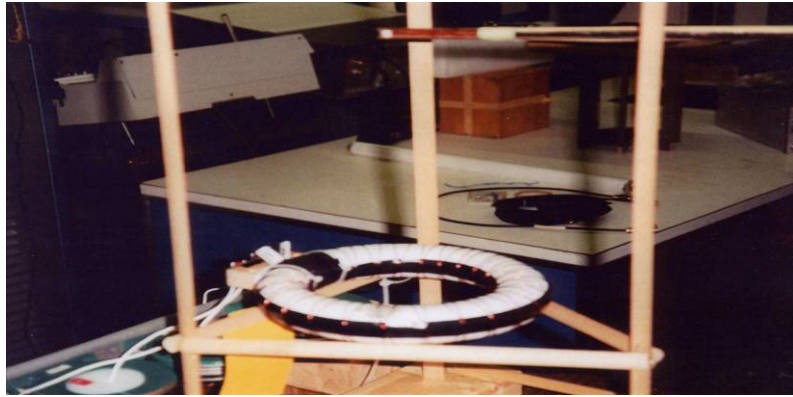
Figure 6. Magnetic probe used to measure magnetic fields generated by transmitting toroids at resonant frequencies.

Figure 7 shows steep magnetic field gradients forming over tightly-wound toroidal coils that may be emitting SU(2) EM radiation. Shown is higher magnetic field peak for the smaller diameter toroid in current-opposing mode and higher magnetic field peak for the larger diameter toroid in a current-adding mode. This could be due to different toroid diameters or different resonant frequencies or both. Of interest were current-opposing modes of operation for the toroids. For, despite no net current flow or magnetic field inside the coils, magnetic fields formed outside them for this mode. Such field patterns appear impossible for ordinary U(1) EM fields - but they are possible for higher order SU(2) EM fields. Also of interest, was formation of circumferential standing waves of magnetic energy over toroids in a current-adding mode. Eight peaks and nulls occurred for standing waves formed on the smaller diameter toroid surface. Ten peaks and nulls occurred for similar standing waves that formed over the larger toroid's surface.
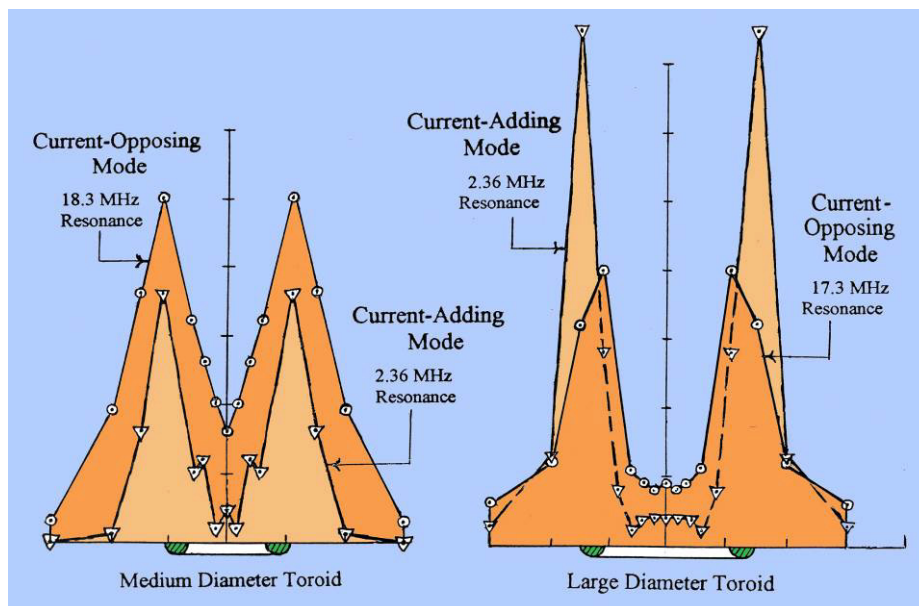
Figure 7. Steep magnetic field gradients forming in the radial direction over tightly-wound toroidal coils.

Figure 8 shows EM magnetic field energy focused into a 'forward direction' from a planar, asymmetric, teardrop-shaped toroidal coil at one of its several resonant frequencies for a current-opposing mode. Such forward focusing might be favorable for applications such as supersonic drag and sonic boom reduction, where work such as Bedin and Mishin (1995) show that thermal and plasma-dynamic effects of EM discharges can reduce aerodynamic drag.
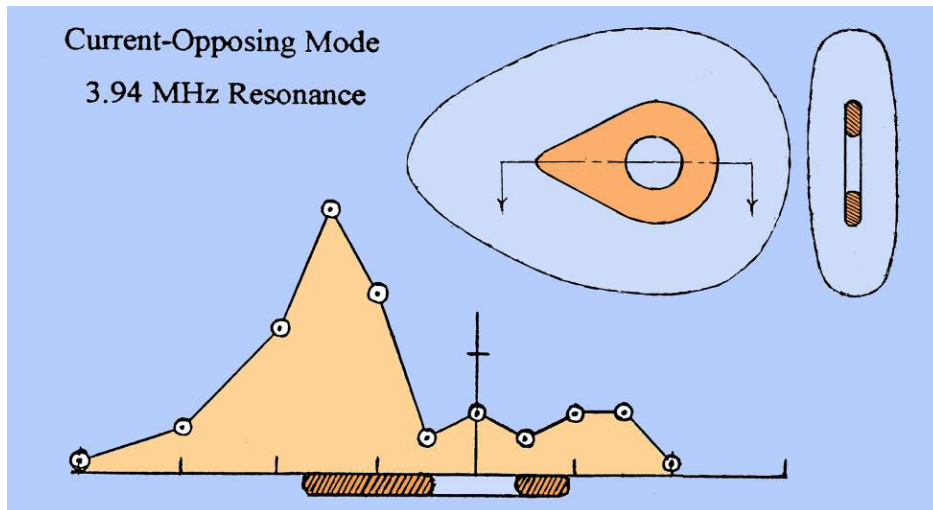
Figure 8. Forward focusing of magnetic field energy from asymmetrical toroids.

As with the small and large diameter circular toroids, standing waves of magnetic field energy formed over the planar, teardrop-shaped toroid when it was radiating in a current opposing mode. However, the standing wave pattern was much more irregularly distributed and both nodes and peaks were difficult to locate with any precision. Magnetic field strength variation with range was measured in one direction out to 10 meters of distance from the large diameter toroid's center in current-adding and current-opposing modes of operation – as is shown in Figure 9. Consistent data was obtained for current-adding mode but less satisfactory data was obtained for current opposing.

Figure 9. Toroid test setup for measuring magnetic field to 10 meters of range.

Figure 10 shows fall-off in EM field intensity from the larger diameter toroid at: a radiating resonant frequency of 1.20 MHz, and in a current-opposing mode. Measured fall-off in signal strength out to 10 m. from the toroid center deviated somewhat from the $1/R^2$ fall-off in signal strength expected for far-field propagation. But all measurements were well inside the near-field of the ~250 m. wavelength associated with 1.2 MHz resonant frequency. A less rapid fall-off than $1/R^2$ occurred at very short distances and more rapid fall-off than $1/R^2$ occurred at the longer distances.
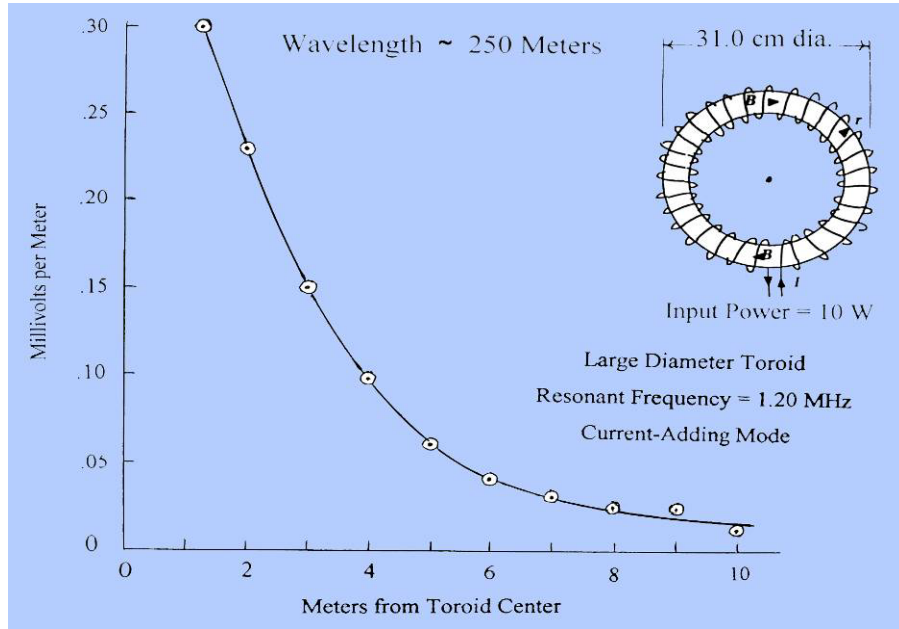
Figure 10. Signal strength fall-off with range for the larger diameter toroid in its current-adding mode.

CONCLUSIONS FROM INITIAL TOROID EXPERIMENAL WORK

Two brief test series have experimentally explored the ideas of Barrett (1998) which suggest that higher order SU(2) EM radiation can be emitted from a toroidal coil when alternating current flows through it at any of the resonant frequencies that can occur for the toroid's geometry. These tests did not prove that SU(2) EM radiation fields were ,indeed, emitted from the tested toroidal coils. But, they revealed interesting and unexpected magnetic phenomena and some appeared consistent with emanation of the SU(2) electromagnetism that was predicted by Barrett (1998).

Our tests could not confirm SU(2) EM field emission from the tested toroidal coils because our ordinary antennas were not capable of detecting the distributed phase patterns of SU(2) A potentials or SU(2) fields. Such detection would have required much more expensive and complex detectors - such as Josephson Junctions - that could detect (but not disturb) the phase patterns associated with states of such fields. Nevertheless, our ordinary U(1) detectors (magnetic probes) detected U(1) magnetic fields outside all tested toroids at resonant frequencies. Such magnetic field detection by our probes would not be expected outside current carrying coils - where only un-detectable U(1) A potentials should exist. But it would be expected if probe presence causes symmetry-breaking of SU(2) fields outside the toroids into U(1) fields. For this would enable detecting the B field components of these U(1) EM fields.

A small number of measurements during the tests indicated significantly stronger signal strength when toroids radiated at resonant frequencies. But there was insufficient test time for detailed exploration of "off-resonance" conditions. This prevented better understanding of what happens electrically inside transmitting toroids and what happens electromagnetically outside them as their resonant frequencies are approached and reached and surpassed. Thus, lack of time for checking or comparing resonance and off-resonance results makes it conceivable that some of our results could ultimately be explained by known U(1) electromagnetism and its U(1) vector and scalar potentials.

However, the most difficult results to explain away are probably those for the current-opposing modes of operation, where counter-flowing alternating currents in contra-wound toroidal coils resulted in no magnetic field whatsoever inside the coils – while, at the very same time, magnetic fields and strong magnetic gradients formed outside them.

FUTURE TOROID TESTING WORK

More testing, involving better field isolation and leakage field considerations, is needed for definitive conclusions on emission of conditioned EM fields from toroidal coils at resonant frequencies and signal benefits they can provide over non-resonant operation. This could be done at places like Hathaway Consulting Services facilities, which now includes an anechoic chamber that will improve the accuracy of any toroid field patterns measured in future testing.

Testing would entail fairly extensive field pattern measurements on only several toroidal coils, with emphasis on an accurate resolution of what happens as resonant frequency is approached and traversed and surpassed. More far-field measurements and determination of the effects of enclosures and magnetic shielding on emitted signal would also be desirable. If results are positive, direct detection of SU(2) fields with Josephson Junctions can also be considered.

ACKNOWLEDGMENT

REFERENCES

Barrett, T. W., "Topological Foundations of Electromagnetism," *World Scientific*, (2008).

Barrett, T. W., "Toroid, Conditioner of Electromagnetic Fields into (Low Energy) Gauge Fields," in the proceedings of the *Progress in Electromagnetic Research Symposium 1998 (PIERS' 98)*, Nantes France, (1998).

Barrett, T. W., "The toroid antenna as a conditioner of electromagnetic fields into (low energy) gauge fields," *Advances in Physics, V. V. Dvnglazov, (ed.)* Nova Science, New York, (2000).

Bedin, A. P. and Mishin, G. I., "Ballistic Studies of the Aerodynamic Drag on a Sphere in Ionized Air," *Pis'ma Ah. Tekh. Fiz*, **21**, (1995), pp. 14-19.

Experiments with Coler Magnetic Current Apparatus

Thorsten Ludwig

German Space Energy Association (DVR) and Berlin Institute for Innovative Energy and Propulsion Technologies (Binnotec), Bouchéstr.12
12435 Berlin, Germany
+491716280357; DrLudwig@thorstenludwig.de

Abstract. Experiments with a replica of the famous Coler "Magnetstromapparat" (magnetic current apparatus) were conducted. The replica was built at the same institute at the Technical University of Berlin where the original was tested by Prof. Kloss in 1925. The details of the setup will be presented in this paper. The investigation of the Coler device was done with modern methods. The output was measured with a digital multi meter (DMM) and a digital storage oscilloscope (DSO). The results of the measurements will be presented. Did Coler convert vacuum fluctuations via magnetic, electric and acoustic resonance into electricity? There is a strong connection between magnetism and quantum field radiation energy. The magnetic moment of the electron is in part an energy exchange with the radiation field. The energy output of the Coler apparatus is measured. Furthermore the dynamics of the ferromagnetic magnets that Coler reported as the working principle of his device was investigated with magnetic force microscopy (MFM) and the spectroscopy mode of an atomic force microscope (AFM). The magnetic and acoustic resonance was investigated with magnetic force microscopy (MFM). The connection between ZPE and magnetism will be discussed as well as the perspective of using magnetic systems as a means to convert vacuum fluctuations into usable electricity.

INTRODUCTION

This article will explore a new type of electrical generator which was invented by Hans Coler. First the history and the general description of the device will be given. The historical part will also mention the early tests of the device by the well known German Professors Schumann and Kloss, which are the main reason why this invention is not forgotten. Another important historical fact is the investigation of the device by the British Intelligence Objectives Sub-Committee (B.I.O.S.) and the confidential, later disclosed, positive report of this agency. The investigation was conducted by Hurst and Sandberg. Hans Coler was contracted in 1947 to rebuild his magnetic current apparatus. This work will present the technical design of a replica of such a Coler device and measurements on that replica. The replica was built by students of the Technical University of Berlin in 1998 and 1999 under the supervision of Dipl. Ing. Andreas Manthey. The construction of the Coler device was part of a course in interdisciplinary innovation learning. The student group took up the Coler device because there is a rich source of technical information on the device and another important reason was that the original device was positively tested at the same institute in 1926. An investigation to retrieve the original documents in the archives of the Technical University revealed that the documents were a toll taken by a British firebomb during a air raid on Berlin in 1943. Since Coler also presented some theoretical hints on the working principle of his device, this work will also deal with the fundamental properties of magnetism and the feasibility of using electrical and magnetic resonances of ferromagnetic magnets to construct a generator. This article will also present an experimental technique that allows testing Coler´s statements on magnetism. The work on magnetism is still ongoing. This work on the Coler generator was taken up because of the credible witnesses for a proof of principle for a device that works with permanent magnets and no other input power. Since the magnetism of the electron can be explained as a relativistic quantum effect with corrections due to the exchange of energy with the zero-point energy quantum fluctuations and permanent magnetism is today seen as a collective electron phenomenon, Coler seems to be good starting point for

practically testing the possibility of using magnetism to convert ZPE into useable electric energy. This connection will be laid out in more detail in a later part of this paper.

A major part of the work presented here is the investigation into the nature of magnetism with modern methods such as magnetic force microscopy (MFM) and the origin of magnetism (Berman *et al*., 2006). Permanent magnets are today understood as a collective phenomenon of the electron spin and the magnetic moments of the electrons involved (Auerbach, 1994). The magnetic moment of the electron is a quantum field phenomenon (Maggiore, 2005).

In order to unveil the working mechanism of the Coler generator two approaches are combined in this paper. On the one hand it was tried to replicate Coler´s magnetic current apparatus and to conduct modern measurements on the replica. In addition another avenue was followed to single out the working principle with modern methods to find the resonance between ferromagnetism and electrical oscillations that Coler gives as a reason for output energy of his device.

THE COLER GENERATOR

Hans Coler was the inventor of two devices by which electrical energy may be derived without a chemical or mechanical source of power. The devices are called the "Magnetstromapparat" (magnetic current apparatus) and the "Stromerzeuger". The "Magnetstromapparat" was developed by Coler and von Unruh early in 1933. With this device, consisting only of permanent magnets, copper coils, and condensers in a static arrangement he showed that he could obtain a tension of 450 mV for a period of some hours. This device consists of six permanent magnets wound in a special way so that the circuit includes the magnet itself as well as the winding. These six magnet-coil combinations are arranged in a hexagon and connected in a circuit which includes two small condensers, a switch, and a pair of solenoid coils, one sliding inside the other (Hurst, 1956).

The "Stromerzeuger" consists of an arrangement of magnets, flat coils, and copper plates, with a primary circuit energized by a small battery. Coler and von Unruh made up a slightly larger model with an output of 70 watts.   This was demonstrated to Dr. F. Modersohn, who obtained from Prof. Schumann and Prof. Kloss confirmation of their tests in 1926. The device was seen by the professors Schumann (Munich), Bragstad (Trondheim) and Knudsen (Copenhagen). Reports by Prof. Kloss (Technical University Berlin) and Prof. Schumann (Technical University Munich) are credential evidence that the device was real and worked. Prof. Schumann is still widely known for the discovery of the Schumann Resonances in the earth atmosphere. Coler then in 1937 built a lager version with an output of six kilowatts.

Since an official interest was taken in his inventions by the German Admiralty the British intelligence started an investigation, although normally it would be considered that such a claim could only be fraudulent. Coler was visited and interrogated. He proved to be co-operative and willing to disclose all details of his devices. He built a "Magnetstromapparat" in 1947 using material supplied to him by the British intelligence (Ministry of Supply), and working only in their presence. The greatest tension obtained with this "Magnetstromapparat" was stated to be 12 volts.

Coler had no complete scientific explanation for the working of his device. He stated that his researches into the nature of magnetism had lead him to conclude that ferromagnetism was an oscillating phenomenon, of a frequency of about 180 kilohertz. This oscillation took place in the magnetic circuit of the apparatus, and induced in the electrical circuit oscillations the frequency which of course depended on the values of the components used. These two phenomena interacted, and gradually built up the tension. Coler stated that the strength of the magnets did not decrease during use of the apparatus; and suggested that he was tapping into a new sort of energy hitherto unknown -"Raumenergie" (Space-energy).

Technical details of the Coler replica used in this work

The Coler generator consists of six permanent magnets with coils wound around it and connected to it in a special way. The electric circuit therefore includes the magnets as well as the windings. The six magnet-coil combinations are arranged in a hexagon and connected as shown in Figure 1.
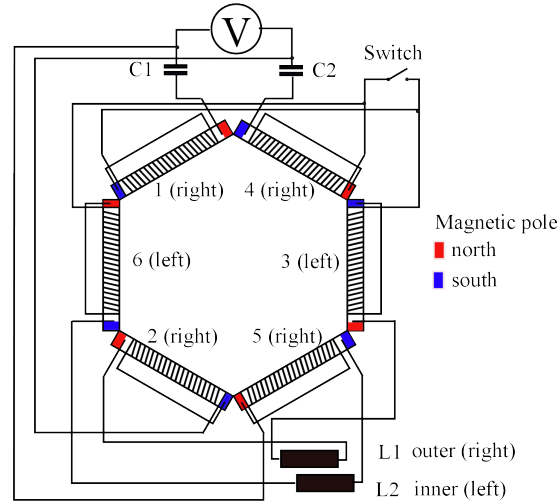
Figure 1. Electric diagram of the Coler magnetic current apparatus.

The circuit includes two small capacitors, a switch, and a pair of air coupled solenoids (L1 and L2) one sliding inside the other. The values of the capacitors were 4.7 nF each. The Coler replica used in this work is shown in Figure 2.
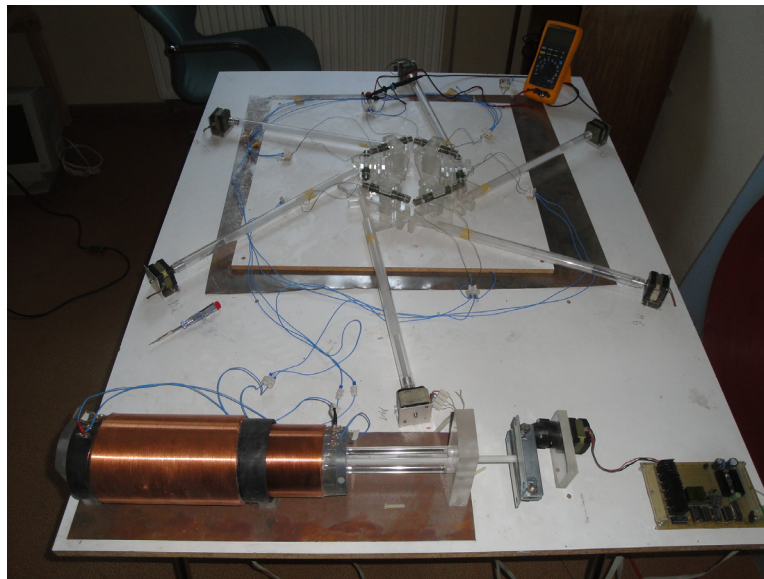
Figure 2. Coler replica used in this work.

One of the important uncertainties of the Coler generator are the material of the magnets and the construction and binding of the coil on the magnets. Some features seam to be schematic other not. It is unclear if the coils should be wound over most part of the magnets as in Figure 1 or only on the edges. The student team decided to wind a homogeneous coil that is soldered and bind as described in the British intelligence report, as seen in Figure 3. The

Magnets were especially manufactured for the original TUB project by IBS Magnet in Berlin. The length of the magnets is 100 mm and the average remanent magnetisation is 200 mT. The magnets were cut and turned to a length of 100mm and a diameter of 15 mm out of a special pure iron. After machining the iron rods were magnetized by IBS Magnets.
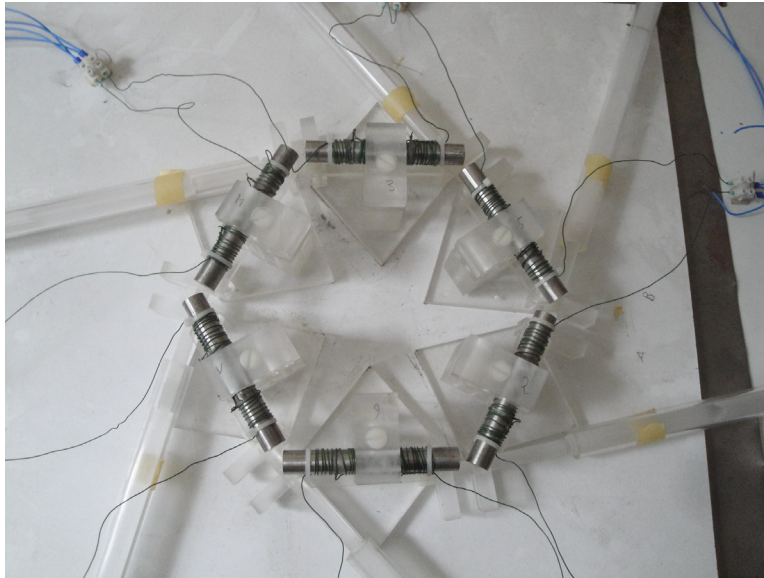
Figure 3. Close up of the magnet hexagon.

The stepper motors seen in Figure 2. are part of the original concept design of the Coler replica. It was planned in 1998 at the TUB to let a computer program find the optimal position of the magnets automatically. The computer and the program could not be retrieved. Electrical and magnetic properties of the permanent magnets and coils used in these experiments are shown in Table 1. Numbers correspond to numbers of the magnets-coil combinations in Figure 1.

Table 1 Electrical and magnetic properties of the permanent magnet-coil combinations.

Magnet-coil	Resistance	Magnetic field at pole
1	0.386 (0,001) Ω	N: 200, S: 180 mT
2	0.232 (0,001) Ω	N: 180, S: 180 mT
3	0.440 (0,001) Ω	N: 170, S: 200 mT
4	0.310 (0,001) Ω	N: 200, S: 180 mT
5	0.385 (0,001) Ω	N: 200, S: 200 mT
6	0.416 (0,001) Ω	N: 180, S: 200 mT

INVESTIGATION OF MAGNETIC AND ELECTRIC PROPERTIES IN THE COLER "MAGNETSTROMAPPARAT"

In the report of the British intelligence the following normal start up procedure for the Coler apparatus is given. Before the device is used, it is kept in the zero position for some time. In this position the switch is open and every magnet is touching the next one. To bring the device into operation, the switch remains open, the magnets are moved slightly apart, and the sliding solenoids are set into various positions, with a pause of several minutes between adjustments. The magnets are then separated still further, and the sliding solenoids are moved again. This process is repeated until at a critical separation of the magnets a reaction in form of a higher voltage is seen on the voltmeter. The switch is than closed, and the procedure is continued more slowly. The tension is then suppose to build up to a maximum where it remains.

A maximum voltage of 133 mV was observed. In the closed position the output voltage was 0.012 mV ac and below 0.00 mV dc. In most positions of the magnets the output voltage was 2-3 mV ac and dc. In a few cases the voltage went up for some minutes to 15 mV, 20 mV, and 46 mV ac with 6 mV DC. In one case the voltage remained for about 5 minutes at 133 mV. An overview of exceptional high output voltages is given in Table 2.

Table 2. Output voltages.

Time	Output Voltage AC	Output Voltage DC
Closed loop	0.012 mV	0.00 mV
Usual output	2-3 mV	2-3 mV
2-3 min	15 mV	
3 min	20 mV	5-10 mV
3 min	46 mV	6 mV
5 min	133 mV	

The exceptionally high output voltages did not last long enough to close the switch and to go on with the next run up stage. The magnetic field strength at the time of the highest output voltage is shown in Table 3.

Table 3. Magnetic field strength

Position, between	Magnetic Field Strength
1-6	310 mT
6-2	380 mT
2-5	210 mT
5-3	280 mT
3-4	310 mT
4-1	300 mT

The output voltage was measured with a Fluke 189 true RMS multi meter and recorded with digital store oscilloscope DSO-5200A from Voltkraft. The digitization rate was 250MS/s at a 9 bit resolution. The results of the measurements with the Fluke DMM are shown in Table 2. The recording for the 46 mV case is shown in Figure 4.
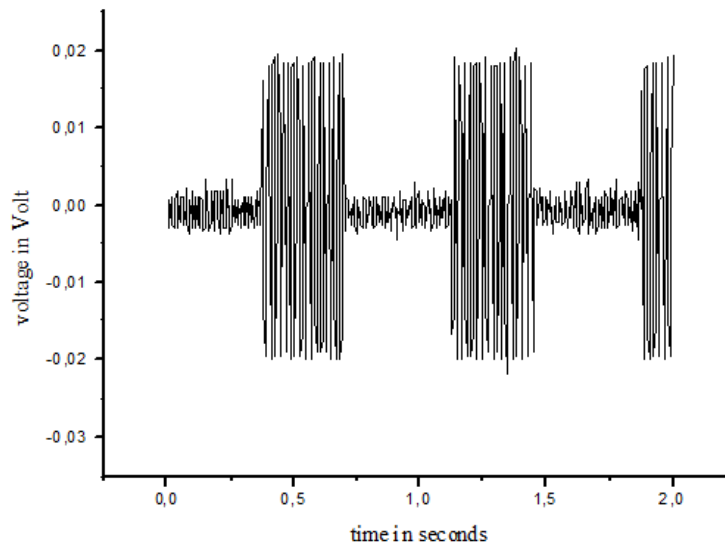
Figure 4. Output voltage over time in the case of 46 mV output voltage.

MAGNETISM AND QED

The magnetic moment μ$_s$ of the electron is given by

$$\mu_s = -g_s \frac{e}{2m_0} s \qquad (1)$$

In equation (1) g_s is the gyromagnetic ratio, e is the elementary charge, s the spin quantum number and m_0 the mass of the electron. In the classical case g is expected to be 1.

The experimental value for g given by Dehmelt (1990) is 2.02319304376(8).

It is one of the most important achievements of the relativistic quantum mechanics that the Dirac equation for an electron in an external field produces almost the right magnetic moment of the electron. The expert is not surprised by this as the magnetic field can be seen as a relativistic effect of the electric field (Schmueser, 1988). The Dirac equation results with a g_s of 2. The difference of the experimental value to g_s is called g-2. The difference can be calculated to a high precision with QED. This process is called radiation correction, as the difference g-2 is the result of energy exchange with the vacuum fluctuations, also called radiation field or zero point energy. Schwinger was the first one to show that the magnetic moment can be calculated from QED (Schwinger, 1948). His result for g-2 is α/π, with α being the fine structure constant. Luttinger showed a simpler way to arrive to this result (Luttinger, 1948). Masperi gives a more qualitative and understandable explanation (Masperi, 1989). These calculations have been experimentally verified for example by the single electron experiment of Dehmelt (1990).

The modern view of the magnetic moment of the electron is that it can be calculated from quantum field theory. The magnetic moment of the electron is partly connected with the vacuum fluctuation because the g-2 part is caused by interaction with the radiation field. Permanent or remanent magnetism is today seen as a collective phenomenon of single electron magnetic moments (Auerbach, 1994). It is therefore justified to investigate permanent magnetism as a means to converts vacuum state energy, into other forms of energy, *i.e.*, electricity. Puthoff and Cole have shown that in principle this energy can be extracted from the vacuum (Puthoff and Cole, 1993). Coler might have found a mechanism that converts zero point energy into usable electricity. He points out that he uses a special resonance of magnetic and electrical vibrations in ferromagnetic material, especially iron. Since ferromagnetism is a collective effect, it can be seen as a self organized dissipative structure. This holds especially for the ferromagnetic resonance. Therefore ferromagnetic materials combine fundamentally vacuum fluctuations and dissipative structures. The self structuring process of the electrons in ferromagnetic material could be a way to cohere vacuum fluctuations. This would make ferromagnetic materials ideal candidates to fulfill the requirements laid out by Moray King for processes that extract energy from the vacuum state (King, 1989). In Order to verify the connection between Coler magnetic current apparatus, magnetism and energy extraction from the quantum vacuum field it is planned to use Casimir force measurements (Ludwig, 2008).

In order to understand Coler´s device and to engineer technology from it, a better understanding of the dynamics of ferromagnetism is needed. Research in magnetic nano-structures, ferrofluids, single spin magnetic resonance force microscopy and magnetic semiconductors promise to lead to these needed new insights.

TEST OF COLER´S THEORY OF FERROMAGNETISM WITH MAGNETIC FORCE MICROSCOPY (MFM)

Coler´s suggestion that ferromagnetism is a fluctuation phenomenon with a frequency around 180 kHz was studied using magnetic force microscopy. In order to achieve this; an ANFATEC standard AFM was equipped with chromium-cobalt coated silicon cantilevers. With this method very small variations in the magnetic properties can be detected. The method is suitable to study changes in the magnets. Experimental method and data will be presented in this section.

Magnetic Force Microscopy

Magnetic force microscopy (MFM) is a special mode of atomic force microscopy (AFM). In MFM a ferromagnetic

tip is scanned at a certain constant height of several ten nanometres above the surface. This mode is also called fly mode. In fly mode first the line is scanned in AFM dynamic mode and then the same line is scanned at a height of several ten nanometers above the topography just measured in the AFM mode. At that height there is no atomic force between the tip and the surface but the strength and orientation of the magnetic field of the surface can still create a force on the ferromagnetic tip. Figure 5 (a) shows the working principle of an AFM. A thin silicon cantilever is scanned line by line over a sample surface. The nm resolution for the scan is achieved with a piezo actuator. The piezo actuator can be positioned in 3 dimensions (xyz) with medium voltage. The force on the tip and therefore on the cantilever is measured with a laser beam that is reflected on the back of the cantilever and a segmented photodiode. If a force is supplied to the cantilever, the cantilever bends, which lead to a shift of the position of the laser beam on the photodiode. If the image is acquired with the tip touching the surface it is called contact mode AFM. If the cantilever is vibrated with tip just above the surface and the force is measured as a change in amplitude or phase shift between driving frequency and photodiode signal it is called dynamic mode AFM. For MFM the AFM is usually used in dynamic mode. Figure 5 (b) shows the MFM imaging with the fly mode. Figure 5 (a) shows the working principle of an AFM which is used in MFM to record the surface topology and Figure 5 (b) shows the working principle of the MFM mode of an AFM which is used for imaging the magnetic properties of the sample. To scan the magnetic properties the cantilever and tip are coated with a Cr-Co layer.
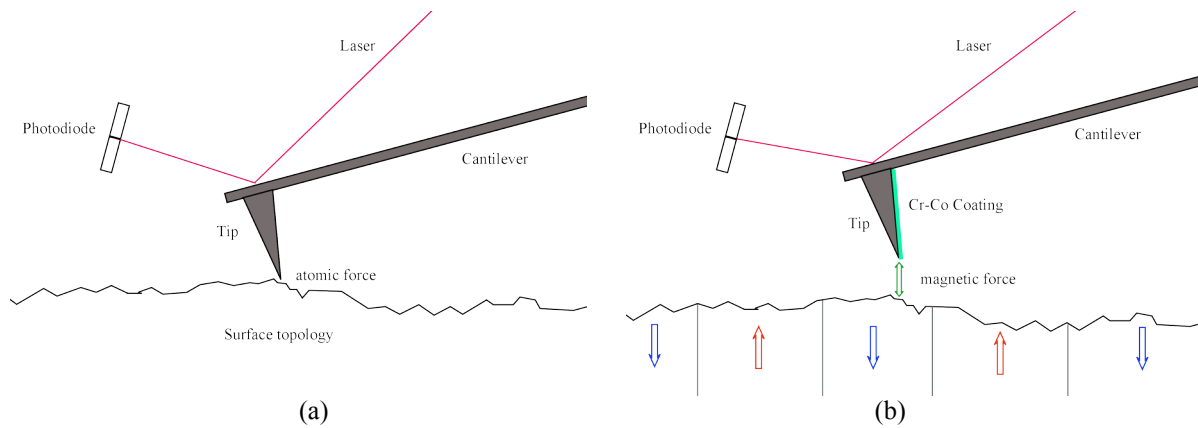
Figure 5. (a) Working principle of an AFM, and (b) of the MFM mode.

The AFM used for the here presented work is shown in Figure 6.
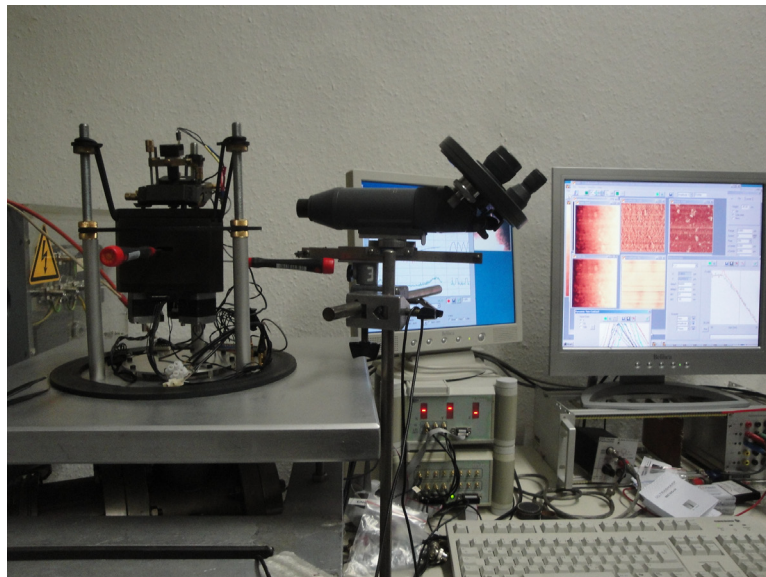
Figure 6. The atomic force microscope used in this work.

In our case the silicon cantilever is 230 µm long, 40 µm wide and 3µm thick. The resonance frequency is 81 kHz and the force constant is 3.5 N/m. The tip and both sides of the cantilever are coated with continuous films of cobalt 1st layer with a thickness of 60 nm and a 2nd layer of chromium with a thickness of 20 nm. The Cr layer is for protecting the cobalt layer chromium. Figure 7 shows a MFM image of a test structure. In the MFM image there is no trace of the topography, which is shown in Figure 8. The topography image was taken with the normal dynamic mode of the AFM. The MFM image shown in Figure 7 was taken in fly mode at a height of 45 nm. The test structure was a piece of a ZIP 100 MB disk. The scanned area was 8 by 8 µm. The tip has a radius of less than 10 nm. The resolution of the images is 5 – 10 nm.
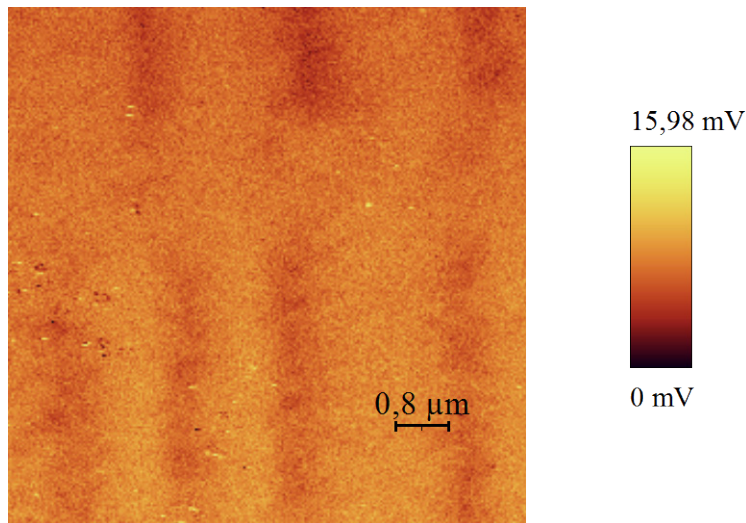
Figure 7. MFM image of the magnetic field strength of a test structure
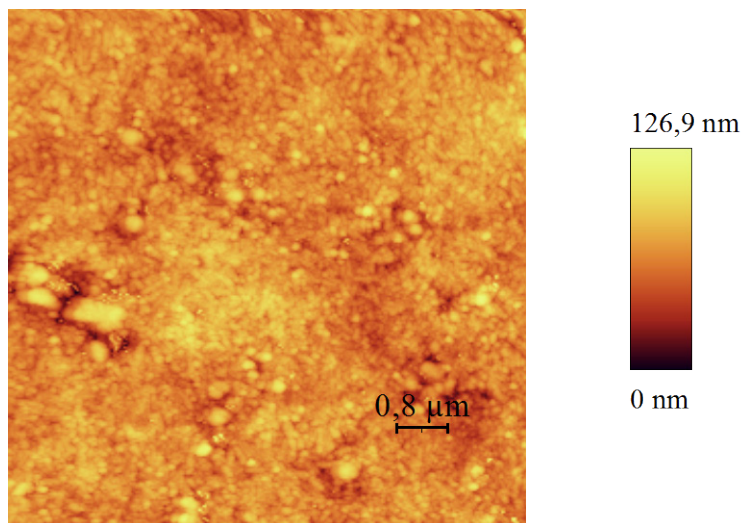
Figure 8. Topography image of the same area as in Figure 7 acquired with AFM in dynamic mode.

MFM Study of Iron Samples

In order to study Coler´s theory iron was scanned with MFM to acquire pictures of the magnetic strength distribution and its dynamics. In Figure 9 an image of an iron plate is shown. In this case the phase angle between

driving force and the photodiode signal was used for contrast.
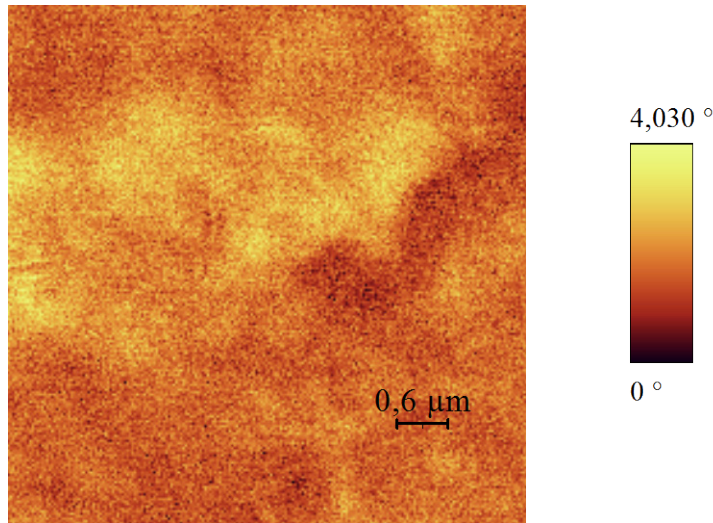
Figure 9. Magnetic field strength of iron in phase contrast.

In order to verify Coler´s hypothesis of the 180 kHz oscillation in ferromagnetic material the spectroscopy feature of the AFM was used. In this case the tip with Cr-Co coating was positioned just above the surface and the photodiode signal was scanned from 20 kHz to 400 kHz. The result of this frequency scan is shown in Figure 10.
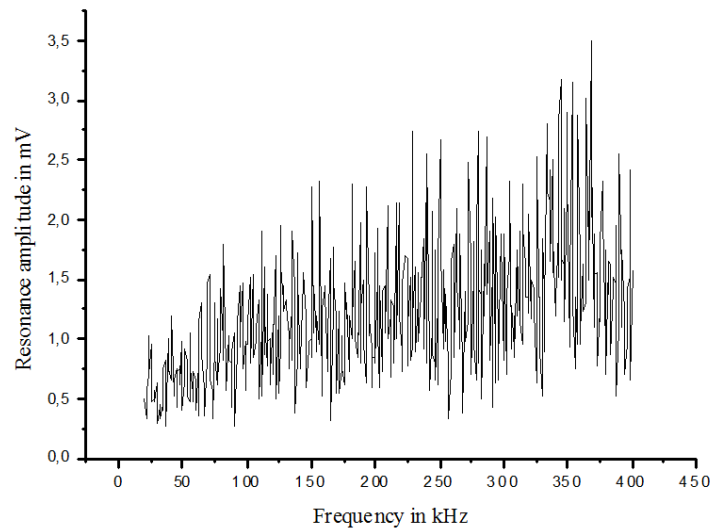
Figure 10. Frequency scan of ferromagnetic iron sample.

So far no clear evidence of a ferromagnetic oscillation phenomenon around 180 kHz could be found. The presented data are to be seen as samples to demonstrate the experimental methods used. It constitutes by no means a complete investigation of ferromagnetism. The investigation of iron samples and iron permanent magnets has to be continued. Of special interest is the measurement of permanent magnets in the magnetic and electrical resonance in Coler´s circuit. This still remains to be accomplished.

CONCLUSIONS

The origin of excess power obtained via magnetic resonance was investigated in the case of a replica of the Coler generator. Even though a maximum of 133 mV and at times 20 to 40 mV could be detected the conclusion is that the

Coler magnetic current apparatus could not be set into function as it was reported by Hurst in the British intelligence report. Since Hurst and Coler point out that it is difficult to hit the right resonance position this is not surprising. The work on the replica is not completed. There are still a number of parameters that can be varied. In addition it is planned to do the same measurements on another replica from a Technical University. The AFM and MFM measurements have also not brought a breakthrough insight into Coler´s claims. The resonance frequency of 180 kHz was investigated by the means of magnetic force microscopy. Therefore no clear mechanism on how the quantum field fluctuations could supply the energy to drive the circuit via the magnetic moment of the electron could be identified to this day. It has to be mentioned that the work is still ongoing and it is hopped to refine the measurement techniques and sample preparation to find definitive results in the future. It is planned to study the same permanent magnet material with the MFM that is used for the magnets in the circuit. Furthermore it is planned to prepare smooth pure iron samples to study the ferromagnetic dynamics in iron. It seems promising to follow up the methods laid out in this work to learn more about the nature of ferro- and permanent magnetism and the possibility to convert radiation field energy into electricity.

ACRONYMS

AFM	–	Atomic Force Microscope
B.I.O.S.	–	British Intelligence Objectives Sub-Committee
DSO	–	Digital Storage Oscilloscope
DMM	–	Digital Multi Meter
MFM	–	Magnetic Force Microscope
QED	–	Quantum Electro Dynamics
RMS	–	Root Mean Square
TUB	–	Technical University of Berlin
ZPE	–	Zero Point Energy

ACKNOWLEDGMENTS

REFERENCES

Auerbach, A., *Interacting Electrons and Quantum Magnetism*, Springer, New York, (1994).

Berman, P. G., Borgonovi , F., Gorshkov V. N. and Tsifrinovich, V. I., *Magnetic Resonance Force Microscopy and a Single-Spin Measurement*, World Scientific Pub., Singapore, (2006).

Dehmelt, H., "Experiments with an Isolated Subatomic Particle at Rest," *Rev. Mod. Phys.*, **62**, (1990), pp. 525-530.

Hurst, R., "The Invention of Hans Coler, relating to an alleged new Source of Power" *B.I.O.S.*, Final Report No.**1043**, Target Number: C31/4799, [declassified], (1956).

King M., *Tapping Zero Point Energy*, Paraclete Publishing, Provo UT, (1989).

Ludwig, T., "Casimir force experiments with quartz tuning forks and an atomic force microscope (AFM)" *J. Phys. A Math. Theor.*, **41**, (2008), p. 164025.

Luttinger, J. M., "A Note on the Magnetic Moment of the Electron," *Phys. Rev.*, **74**, (1948), p. 893.

Maggiore, M., *A Modern Introduction to Quantum Field Theory*, Oxford University Press, Oxford, (2005).

Masperi, L., "Qualitative description of the electron's anomalous magnetic moment," *Revista Brasilleira de Fisica*, **19**, (1989), p. 215.

Puthoff, H. E. and Cole D. C., "Extracting energy and heat from the vacuum," *Phys. Rev. E*, **48**, (1993), p. 1562.

Schwinger, J. S., "On Quantum-Electrodynamics and the Magnetic Moment of the Electron," *Phys. Rev.*, **73**, (1948), p. 415.

Schmueser, P., *Feynman-Graphen und Eichtheorien fuer Experimentalphysiker*, Springer, Berlin-Heidelberg, New York, (1988).

Water Electrolyzers and the Zero-Point Energy

Moray B. King

P.O. Box 859
Provo, UT 84601
801-224-1814; mbking42@aol.com

Abstract. The gas emitted from popular water electrolyzer projects manifests unusual energetic anomalies, which include vaporizing tungsten when used in a welding torch and running internal combustion engines on small quantities of the gas. Some claim to run generators in closed loop fashion solely on the gas from the electrolyzer, which is powered solely from the generator. Most investigators believe the energy is from burning hydrogen. A hypothesis is proposed that the dominant energy is *not* coming from hydrogen, but rather it is coming from charged water gas clusters, which activate and coherently trap zero-point energy.

INTRODUCTION

The water electrolyzer projects are popular with inventors and hobbyists worldwide. There are thousands of videos posted on *YouTube* under the search, *water fuel*. Nearly everyone believes their electrolyzers produce a mixture of hydrogen and oxygen gas known by various names such as HHO, hydroxy, oxyhydrogen, and Brown's gas. Yull Brown (1977) is famous for investigating the welding applications of the gas and discovered intriguing energetic anomalies (Wiseman, 1998). The gas exhibits a cool flame, ~130 degrees C, yet it can vaporize tungsten, a feat beyond today's commercial welding torches (Wiseman, 2001). The academic community has yet to explore or explain this anomaly. Burning hydrogen cannot account for it.

Perhaps the most popular application of the water electrolyzers is to boost an automobile's gasoline mileage (Kelly, 2008; Panacea, 2010). An energy anomaly manifests here as well for the boosters typically produce only a few (5-20) liters of uncompressed gas per minute. Yet many claim significant increase in miles per gallon (20 – 50%). Burning hydrogen cannot account for it.

Even more surprisingly some investigators have claimed to run gasoline generators on 5 to 6 liters per minute of the uncompressed gas, and the generator's electrical output was stable on the order of a kilowatt (Allan, 2009, 2010). Such claims appear remarkable, considering the low efficiency of typical internal combustion engines (~20%). Burning hydrogen certainly cannot account for this.

This paper will explore the hypothesis that the dominant energy coming from the water electrolyzers is not from hydrogen, but rather it is from another source which might be far more energetic: charged water gas clusters, which activate and coherently harvest zero-point energy (ZPE). Others have proposed a coherent water zero-point energy interaction. Prevenslik (2001) introduced a model where a collapsing nano bubble coherently activates a standing wave from the ZPE whose continuously increasing resonant frequency acts like an ultraviolet to x-ray laser which coincides with the dissociation frequency of the water's hydrogen-oxygen bond to yield charge separation. He applied the model to explain steam electricity, waterfall ionization, sonoluminescence, and thundercloud charge separation. If Prevenslik is correct, it implies the zero-point energy significantly contributes to lightning formation. Appendix A summarizes the author's hypothesis (King, 1989, 2001) on how the zero-point energy might coherently participate in self-organized collectives involving ionized matter or plasma.

To further support the ZPE hypothesis, another phenomenon that exhibits energetic anomalies similar to Brown's gas is discussed in Appendix B: plasma charge clusters. Plasma charge clusters are a form of microscopic ball lightning that have been experimentally observed and extensively studied by Ken Shoulders (1991). He named them "electrum validum" (EV) meaning "strong charge," and later renamed them "exotic vacuum objects" (EVO) when he became convinced that they coherently coupled to the ZPE to account for the excessive energy they manifested (Hasslberger, 2007). The observed energetic anomalies in their interaction with high melting point ceramics are similar to those exhibited by the Brown's gas welding torch.

BROWN'S GAS ANOMALIES

Brown's gas exhibits energetic anomalies that have not yet been addressed by the scientific community. The most frequently observed anomaly occurs in welding applications. Here the burning gas exhibits a cool flame measured to be about 130 degrees C, cool enough to quickly pass one's hand through it (Wiseman, 2001). The flame does not boil water by direct contact, yet when it interacts with metal, it readily melts it. It has been shown to even sublimate (and oxidize) tungsten. Commercial welding torches cannot vaporize tungsten.

Recent university studies by Eckman (2010) confirmed the low temperature of the Brown's gas flame as well as its ability to sublimate and oxidize tungsten. A mass spectrometer was used to determine the constituents of the gas, and he discovered the gas contains little hydrogen of either mono-atomic or diatomic form. Instead he found the gas to be predominantly clusters of water in a gaseous form that contained excess electrons. This observation matches the literature that discusses an observed form of water clusters known as "hydrated electrons" (Neumark, 2004), where experiments have determined that the excess electrons are trapped in the interior of the cluster. Eckman suggests that at the heart of the cluster there exists a linear isomer of the water molecule where the excess electrons are held in the d orbitals of the oxygen atom. Here the cluster might be a form of Rydberg matter where nearby molecules in the cluster shares the high-energy band electrons. Eckman's hypothesis was inspired by a preliminary x-ray diffraction image showing a linear water molecule shape, but further studies must be completed to confirm it. The Rydberg matter hypothesis offers a coherent storage mechanism to hold excess energy in a gaseous charge water cluster.

Wiseman (1998) has gathered a repository of research about Brown's gas. Perhaps the most astounding anomaly claimed involves replication of Yull Brown's experiments to alter the radioactivity of americium (Wiseman, 2007). The experiment involves impinging the welding flame onto a mixture of aluminum and iron (akin to thermite) on which sits the americium sample. The flame triggers a small explosive event, after which the americium sample exhibits little radioactivity. There are similar experiments involving EVO strikes (Shoulders, 2004) as well as high-energy plasmoid strikes (Adamenko, 2004) into pure metallic targets that manifested transmutation into elements whose isotopes are not readily found in nature (see Appendix B). Just like plasmoid strike events, could the abrupt explosive interaction of the Brown's gas charged water clusters with the thermite alter the nuclei of the radioactive sample? Such experiments would have to be extensively and carefully repeated by the academic community before concluding that element transmutation is occurring. If such events could be repeatedly demonstrated, it might imply a coherent ZPE interaction with atomic nuclei to account for an energy density sufficient to influence the nucleus.

The charge water gas hypothesis gains further support from observation of electrolyzer bubbles between the parallel plate electrodes. When the plates are separated over a cm, near the cathode are observed the hydrogen bubbles and near the anode are observed the oxygen bubbles as in standard electrolysis. However, in the gap between them are observed a third set of bubbles that contain the more highly energetic gas that Wiseman (1999) suggested to be "electrically expanded water," which is essentially the same as the charged water gas cluster hypothesis here. This is the pure form of the gas, which is the source of the energetic anomalies. Suartt and Gourley (2008) have filed a patent, where they further separate the electrodes so that they can harvest just the middle set of bubbles, and eliminate hydrogen from the mix. The pure gas still exhibits all the welding anomalies, and they are able to safely store it under pressure because it contains no hydrogen. With the electrodes so widely spaced, Suartt and Gourley had to add extra electrolyte to their water and conduct appreciable current to generate the gas, which prevents them from exhibiting any net energy gain. Nonetheless, they have developed a technique to harvest the pure form of the gas for repeatable study that might be intriguing to the scientific community: a form of water that "burns" with coherent energetic content sufficient to vaporize tungsten.

VIBRATING THE WATER

Another technique for making the pure form of the charge water cluster gas might have been invented by Ohmasa (2009). Ohmasa subjects the water to mechanical vibration at ~100 Hz by a set of paddles to dramatically lessen its surface tension. Even if detergent is added to the water, it will not form visible bubbles during vibration. Ohmasa states that bubbles are forming at nano scales, which are not visible to the naked eye. When the water is electrolyzed, he produces abundant gas that exhibits all the anomalies of Brown's gas, yet it apparently contains little free hydrogen for he can likewise safely store the gas under pressure for long periods of time (over two years), after which the gas still exhibits its energetic form when ignited. Ohmasa was able to run an internal combustion engine with just the gas, while blocking any extra air intake into the engine. Ohmasa claims that vibrating the water lowers its surface tension to make nano bubbles, which yields a superior, more energetic form of the water gas from the electrolyzer.

It appears that Chambers (2000) inadvertently discovered an efficient means to vibrate water in an electrolyzer. Chambers used a toroidal coil (1500 turns of wire on a ferrite core) under water in his electrolyzer, and drove it at ~19 Hz. The gas from the electrolyzer exhibited a superior burning characteristic that allowed him to directly use it to fuel a 1 KW Honda generator without needing to adjust the timing on its internal combustion engine. Chambers believed his electrolyzer was producing parahydrogen via the coil's magnetic field because the gas would burn slower than natural hydrogen. When he did not use the coil, the electrolyzer emitted gas that would burn faster, which he assumed was orthohydrogen. It is unlikely that the coil's magnetic field influenced the water since the field lines are effectively confined inside the ferrite toroid. In view of Ohmasa's discovery, we can now infer the actual purpose of the coil: The alternating magnetic field has a corresponding alternating vector potential surrounding the coil, which in turn induces an oscillating, toroidal electric field around the coil. The charged water clusters created in the electrolyzer would then oscillate with the electric field causing the water to vibrate at the drive frequency. Like Ohmasa discovered, the result of electrolyzing water while it is vibrating produces a superior, more energetic form of water gas.

Many inventors and hobbyists have tried using toroidal coils to make a better gas. Eardley (private communication) used ten ½ inch diameter ferrite toroidal coils with 25 windings of 4 gauge wire on each and mounted them on a circuit board as two groups of five coils, each group connected in series. He drove one group with low frequency pulsed DC square waves at 12 volts, 30 amps and the other group at 35 amps (because that was the maximum rating of the coils). He drove his electrolyzer with pulsed DC square waves at 12 volts, 10 amps. The electrolyzer consisted of 25 parallel plates (304L stainless steel, 16 gauge, 8 inch x 11 inch, with 1/8 inch rubber gaskets separating the plates). The electrolyzer emitted sufficient gas to run a lawn mower engine. To investigate the quality of the gas, Eardley filled balloons with the gas emitted from the electrolyzer. It is interesting to note that when the toroidal coils were activated, the gas in the balloon was heavier than air, and the balloon would drop. When the coils were inactive, the electrolyzer gas would be lighter than air, and the balloon would rise. Eardley also isolated the heavier-than-air water gas by storing it overnight in a paper bag. Since the bag is porous to hydrogen, any free hydrogen vents away. The next day he opened the bag, and the residual water gas would not disperse. When lit, it would implode back to liquid water with a distinctive pop. Eardley surmised that the heavier-than-air water gas contained little free hydrogen, and he would then contain the gas under medium pressure (~50 psi) in order to drive larger internal combustion engines.

Eardley recently tried experiments where the water was constantly circulated through the gaps between the electrolyzing plates via a small pump (powered at 12 volts, 8 amps toggled off and on each second to maintain a circulation water pressure of ~25 psi). He could then avoid using the toroidal coils entirely. Eardley found that rapid water circulation produced the most gas of all his experiments, and the gas appeared white like fog. He then was able to reduce his total input power to ~200 watts. It appears that charging water that is rapidly flowing multiple times through the inter-electrode gaps integrates the energy content of the water, and yields a more powerful water gas.

Originally for the electrolyte Eardley added a mixture of potassium carbonate (2 teaspoons) plus a little sodium hydroxide (1/2 teaspoon) per gallon of pure water made by reverse osmosis. The potassium carbonate reduces the surface tension of the water, but it is emitted from the electrolyzer along with the water gas. To recover it, Eardley recycled the engine's exhaust water back to the electrolyzer. Later, when Eardley used the water pump instead of the toroidal coils, he found he could omit the potassium carbonate from the solution. However, he still continued to

recycle the engine's exhaust water. Recycling the exhaust water appears to offer an added benefit: There still might exist energetic charged water clusters in the water after discharge in the engine. If so, the clusters would exhibit behavior akin to the "black" EVO (Shoulders, 2000), a plasmoid-like form that seems to be dormant, but can be re-activated with a voltage pulse (see Appendix B). Recycling the exhaust water might allow an effective energy recapture and integration for the system.

Perhaps the simplest means to produce an abundance of charged water gas clusters has been discovered by the inventors and hobbyists whose electrolyzers have very small gaps between the electrodes (less than 1 mm). Here any free hydrogen or oxygen atoms produced on the electrodes tend to join the water clusters forming in the middle. The primary motivation for the small gaps is to reduce or eliminate the use of electrolyte in the water, which allows a significant reduction in drive current and thus input power. It is electrolyzers of this type that have resulted in the claims of excessive energy production.

CONDITIONING THE ELECTRODES

Since water (especially distilled water) does not readily conduct electricity, inventors have learned that they must "condition" their electrodes, which are typically 316L stainless steel. The result of conditioning creates a rough, microscopic sharp pointy surface, which induces high electric fields around the points and facilitates microscopic electric discharges into the water. If the electrodes are not properly prepared, no current will flow, and the electrolyzer will fail to produce any bubbles whatsoever. This is a frequent occurrence for hobbyists when they first begin their research, and they typically add electrolyte (potassium hydroxide or sodium hydroxide) to the water and are then happy to produce gas bubbles. Since most researchers believe they are making hydrogen with their electrolyzers, they naturally want to supply a large drive current to follow Faraday's law, which essentially states you need to supply one electron for each hydrogen atom you wish to dissociate from the water. The inventors that properly condition their electrodes produce an abundance of gas that appears to exceed Faraday's law, but the law is not actually violated because the gas abundance is not from hydrogen production.

Techniques for electrode conditioning have gradually improved as researchers have been sharing their results. Lawton, who was replicating the electrolyzer of Meyer, developed a long protocol by conditioning his electrodes in tap water (Kelly, 2009, p114). He would run a repetitive, hourly sequence of low current to high current for about a month. During the conditioning a reddish brown crud (likely iron oxide) would discharge from the electrodes and the water would have to be periodically replaced. Gradually, a whitish grainy surface would accumulate on the electrodes. The whitish material has not yet been analyzed but it could be salts, carbonates, or silicates present in the tap water. Ravi (2008) who replicated Lawton's electrolyzer was frustrated with no gas production whatsoever until he followed Lawton's conditioning protocol, after which he was able to produce abundant gas using only 0.5 amps of current. Tap water is a poor medium for scientific replication because the water's mineral content is unknown.

Boyce developed a technique that conditioned his electrodes in a mixture of distilled water and potassium hydroxide that took about three days (Kelly, 2008; Panacea, 2010). He first roughened the electrodes by cross-hatching them with sandpaper. Then he conditioned them in the electrolyte solution with DC current. The electrodes would likewise emit a brownish crud, and the water would have to be periodically cleaned. After three days the electrode would exhibit a grayish white surface and then would be ready for use. All researchers stressed the importance of not touching the electrode surface once it is conditioned because it would damage their charge emitting properties

Zigouras (private communication; panacea-bocaf.org; Beene, 2007) discovered a straightforward technique for preparing stainless steel electrode plates. He media blasted them with 40-grit silicon carbide and then cleaned them with an ammonia-based cleaning solvent. No further conditioning was needed. Zigouras stressed it was important to media blast the surface at 45 degrees and not straight on. The microscopic craters from the media blasting would then have sharp edges. Zigouras also had a very tight gap between his plates, 0.6 mm, which allowed him to convert water sucked through the plates nearly instantly into energetic water gas by means of high current. Zigouras exhibited one of the fastest gas producing electrolyzers on the web, and his approach to conditioning the plates offers the opportunity for easy replication.

Eardley (private communication) prepared his 304L stainless steel plates by having a plating company immerse them in hydrochloric acid for 30 minutes, a harsh descaling technique called "pickling." The plates are rinsed with

water, and then immersed in a bath of potassium hydroxide solution where they are electrolyzed at 10 amps for about 45 minutes until they no longer discharged brownish crud. Afterward Eardley immerses the plates in vinegar for 30 minutes, and washes them in a dishwasher using standard (dishwasher) detergent. The hydrochloric acid (especially with residue ferric chloride) aggressively erodes the surface of the stainless steel leaving a microscopically rough, pointy surface that supports electric discharge characteristics apparently favorable for charge water cluster formation. The surface yields abundant gas production from the electrolyzer, and the water remains crud free. Eardley's protocol for preparing stainless steel electrodes offers consistent repeatability for manufacturing high quality electrodes.

Conductive materials that already have a rough dendritic surface might make good candidates for electrodes. Mixed metal oxide titanium has been used in standard commercial electrolysis without any need for preparatory conditioning. It has been successfully tried in some booster water electrolyzer projects (Panacea, 2010), but so far only with large inter-electrode gaps, which requires electrolyte solution and high current. (Since most researchers believe they are making hydrogen, they typically add electrolyte to produce large currents and see no reason to have small gaps between the electrodes.) Other rough materials such as sintered stainless steel have been discussed as good candidates, but so far not yet tried. Most hobbyists use 316L stainless steel because it is cheap, and it has a track record on the worldwide web with many claims of success.

POWERING GENERATORS

There are numerous projects on the web that demonstrate powering small motors and portable generators exclusively from the water electrolyzer's output gas. Ohmasa (2009) shows it in his video, and Chambers' (2000) patent mentions running a 1 KW Honda generator. The goal is to produce enough gas at minimal electrical input to the electrolyzer to make the system self-running where the rectified output from the generator is the sole source of input power to the electrolyzer. This would dramatically prove the existence of a new energy source. At first glance this goal appears ludicrous because the generator's internal combustion engine is only about 20% efficient, and there are other energy losses throughout the closed loop system as well. The net energy content of the hypothesized charged water gas clusters would have to be extraordinary (over 5x the input power) to overcome these losses to manifest a self-running system. Yet there have been announcements claiming to have done so.

Steve Eaton has claimed to have successfully run a closed loop, generator electrolyzer system that produces six liters of gas per minute that even exhibited some excess power to drive external loads (Allan, 2009). He teamed with Jeff Sokol (2009) of Hybrid-Tech Corporation to publish the plans so that others could replicate his results. The electrolyzer cell consists of 27 pairs of 16-inch long cylindrical stainless steel electrodes (1/2 inch outer diameter) with tight spacing (under 1/32 inch). A spiral wrapping of polystyrene line maintains the gap between the cylinders, and it guides the gas into a helical flow as it travels up the gap between the electrode tubes. The power needed to drive the electrolyzer was 12.5 volts, 30 amps DC. The electrolyzer used a weak electrolyte solution (one gram of potassium hydroxide per gallon of distilled water). The gas output was sufficient to run a 3.25 KW Troy-Bilt generator, which not only provided all input electrical power to the electrolyzer, but also had excess power to light a few light bulbs. Construction of the electrode assembly is not easy, and so far no one has claimed a replication success.

In Germany Oliver and Valentin have claimed to run a small 1 KW generator in a closed loop fashion using three Anton cells (Allan, 2010). The commercially manufactured Anton cell consists of seven parallel-plate stainless steel electrodes, whose 1 mm spacing is maintained by neoprene gaskets. The electrolyte solution consisted of 3% potassium hydroxide in distilled water. Approximately 900 watts of input power was required to produce a gas output of 6 liters per minute. Oliver and Valentin had to provide their own timing circuit to properly fire the generator spark plug and avoid igniting a waste spark. The system ran for about 40 seconds in closed loop fashion, but the system was not stable and still requires further circuits to regulate the power fed to the electrolyzer from the generator. An open source project has been started in Germany to promote replication.

Perhaps the most spectacular claim is from Frederick Wells, who claims to have successfully run a truck on just the water gas from his electrolyzer without depleting his battery (Couch, 2010). Wells is now engaged in an "open source" public project to build a self-running generator, electrolyzer system (Allan, 2010 b). His cylindrical

electrode assembly is designed to vibrate at acoustical frequencies, which helps to disrupt the water's surface tension (much like Ohmasa's vibration technique) to produce abundant gas.

DRIVING WITH PULSED DC WAVEFORMS

A number of investigators have found that using pulsed DC square waves to drive the electrolyzer have enhanced gas production. Chambers patent describes exploring the spectrum from 1 to 250 KHz for the square wave frequency. Many researchers have found that driving the electrolyzer with a square wave around 40 KHz yields good results (Kelly, 2008). Most agree that the best drive frequency has to be experimentally discovered for each electrolyzer because there is no one simple frequency that manifests a full system resonance. Zigouras (private communication; panacea-bocaf.org; Beene, 2007) discovered that he had to gradually and continuously alter the drive frequency by a few KHz centered near 40 KHz to optimize gas production. As a waveform improvement, Lawton discovered that a high voltage spike on the leading edge of the square wave increased the energy content of the output gas (Kelly, 2008, p125). Even though successful gas production occurs with a simple DC drive, using pulsing techniques have helped to reduce the need for large input currents.

SUMMARY

This paper was motivated by the apparent success of the researchers and hobbyists in the "HHO community." They have been demonstrating unusual energy anomalies and have been trying to explain them in terms of hydrogen production. Those that are scientifically trained realize that hydrogen cannot account for what is claimed, and thus the discussion groups on the web are engaged in vituperative argument. In a sense, both sides are right: hobbyists appear to be demonstrating energetic anomalies and hydrogen is not the source.

The hypothesis offered is that the single-duct electrolyzers are producing charged water gas clusters, which is the dominant energetic component instead of hydrogen. The electrolyzers that yield the largest energy anomalies appear to make more charged water clusters and less hydrogen. From the study of the disclosures by many inventors, the following characteristics seem to make favorable electrolyzers:

1. Clean, rough electrode surface
2. Small gap between the electrodes
3. Circulate or vibrate the water
4. Minimum electrolyte (typically potassium hydroxide or sodium hydroxide)
5. Driving electrolyzer with pulsed DC square waves
6. High voltage spike on the leading edge of the square wave
7. Recycling the exhaust water back to the electrolyzer

Also it appears that Eardley recently discovered a significant improvement by "pickling" the stainless steel plates in hydrochloric acid to make a microscopically rough surface, and rapidly circulating the water through the inter-electrode gaps to charge it.

CONCLUSION

Since hobbyists typically do not have the equipment to measure the constituents of the gas produced from their electrolyzers, the academic community can help resolve what is happening by an orderly research program. Since the one energetic anomaly that is well established is the vaporization of tungsten by the Brown's gas welding torch, the first step is to confirm this. The second step is to analyze the content of Brown's gas, and then use the appropriate techniques to produce the pure form of the charged water gas. Analyze the gas to show there is no hydrogen content, and then reconfirm that it still exhibits the welding torch anomalies. At this point the scientific community would have a pure energetic anomaly to study: a form of water that appears to "burn" with an extraordinary coherent energy content.

The second phase would be to investigate the energy content of the pure water gas. If it runs a generator, then the generator's output power and the electrolyzer's input power can be measured. If excess energy is measured, then a closed loop system can be attempted. If a closed loop system involving a (internal combustion engine) generator can

idle for a significant time, then a new energy source would be demonstrated. At this point it would be valid for the academic community to consider the zero-point energy hypothesis as a possible explanation.

It is the author's hope that the scientific community would be willing to engage in such a research program. It just might be that the HHO community has inadvertently discovered a surprisingly simple means to tap the zero-point energy.

ACKNOWLEDGEMENTS

APPENDIX A

Can the Zero-Point Energy Become an Energy Source?

Considering that the zero-point energy might be an energy source is an unusual hypothesis. Most of the scientific community outside of the field of physics, know little about it. The majority of the physics academic community would likely reject the hypothesis as too radical a paradigm shift (Kuhn, 1970). However, experts in the field of zero-point energy research realize it is an open question (Cole and Puthoff, 1993; Davis, et al., 2006)

The zero-point energy of vacuum is comprised of fluctuations of intense electromagnetic field energy at the scale of the Planck length, 10^{-33} cm. The Planck length is twenty orders of magnitude below the size of the elementary particles. The name "zero-point" refers to absolute zero degrees Kelvin meaning that the energy is integral to the pure "fabric" of space in the absence of light, heat and matter. Historically the energy was discovered at the birth of quantum mechanics where the modeling required an underlying jitter to all quantum mechanical systems. Dirac showed that the source of the jitter was electric field fluctuations inherent to the fabric of space itself, which could birth electron-positron pairs that spontaneously pop in and out of existence in our three dimensional space (Gamow, 1966). Wheeler's theory of *Geometrodynamics* (1962) showed that the huge energy densities would alter the space-time metric creating Planck size, black hole - white hole pairs that channel electric flux through microscopic channels he named "wormholes." Wheeler's theory implies that the source of the ZPE is effectively electric flux from higher dimensional space that orthogonally penetrates our 3-space brane. As the electric flux passes through our 3-space it produces a seething, chaotic turbulence called the "quantum foam," which manifests behavior akin to turbulent plasma at the sub-quantum scale.

There is a tremendous energy density in the chaos of the quantum foam. Can it possibly be harvested as an energy source? At first the answer appears to be no because the fluctuations are chaotic and appear to be random in their behavior. However, in 1977 Ilya Prigogine (1977, 1984) won the Nobel Prize in chemistry for showing that under certain conditions, a system may evolve from chaos into self-organization. Three conditions are required for a chaotic system to exhibit self-organization: The system must be 1) nonlinear, 2) far from equilibrium, and 3) have an energy or matter flux through it.

A good example of self-organization would be vortex formation during hydrodynamic turbulence. Another example would be vortex or vortex ring pair production arising in turbulent plasma. Bostick (1957) studied plasma vortex rings called "plasmoids" and noted that they tended to form in pairs of opposite helicity, which conserved angular momentum. Plasmoid pair production in turbulent plasma and electron-positron pair production arising in the quantum foam might both exhibit archetype self-organization, the creation of macroscopic order from an underlying microscopic collective. The archetype self-organization supports Nobel Laureate, Robert Laughlin's (2005) thesis, where he contends everything at its foundation arises from the self-organization of collectives including the laws of physics themselves. Collectives in the quantum foam are maintained by the orthogonal electric flux that passes through them, much like the flow of a stream maintains a whirlpool. Jennison (1989) and Turtur (2010) offer models involving this concept. Modeling elementary particles as collectives is dramatically different from modeling them as point entities or Planck length strings. Laughlin's thesis involves a paradigm shift from today's popular particle theories. Such a paradigm shift might be further supported if even larger, macroscopic collectives could be shown to exist.

Can Macroscopic ZPE-Matter Collectives Exist?

The zero-point fluctuations intimately interact with all elementary particles via vacuum polarization. Quantum Electrodynamics describes a coherent cloud of vacuum energetic activity surrounding all particles that gradually declines with distance. There is no real separation of the particle from its vacuum polarized cloud (Senitzky, 1973). In order to theoretically calculate the values for a particle's observed mass and charge, a mathematical renormalization is used to subtract out the high frequency energetic fluctuations to yield the finite values experimentally observed.

The different elementary particles have different descriptions of their vacuum polarization (Scheck, 1983). Electrons, especially those in the conduction band of metals are described as a smeared charge cloud that is effectively in thermodynamic equilibrium with the vacuum fluctuations. No net energetic yield could arise from such a system, which explains why no energy anomalies are observed in standard electrical and electronic circuits. However, an atom's nuclei have steep lines of vacuum polarization converging onto it. This might offer the capability to induce coherence in the zero-point fluctuations by abrupt motion of the nuclei. Exotic coherent vacuum effects are observed in heavy ion collision experiments (Celenza, et al., 1986), but no researchers have attempted to measure excess energy anomalies. However, energetic anomalies are observed when a large number of nuclei abruptly surge in plasma experiments involving the ion-acoustic mode. The energetic anomalies include run-away electrons, high frequency voltage spikes, and excessive heating. The energetic anomalies are often observed in conjunction with the formation of vortices and plasmoids (Watanabe, et al., 2005). Here might be evidence for an organized collective involving plasma particles and ZPE coherence.

APPENDIX B

Plasma Charge Clusters

Ken Shoulders (1991) has extensively studied micron size, plasmoid-like forms resembling microscopic ball lightning that exhibit excessive energy anomalies. He creates them from an abrupt discharge from a known capacitor at a known voltage through a sharp pointed electrode. In the abrupt discharge the microscopic tip of the electrode blows off yielding a pure unipolar discharge event, similar to exploding wire experiments. The plasmoid form travels along groves on dielectrics, and when it contacts a metallic surface, it explodes emitting an electromagnetic pulse (EMP) and bores a crater into the target material. The measured EMP is greater than the input energy from the capacitor, and its ability to bore through high melting point ceramics like aluminum oxide convinced Shoulders that the entity contained excessive energy, and thus he named them "exotic vacuum objects" (EVO) to reflect his hypothesis that the excess energy was from coherently coupling the vacuum's zero-point energy into the plasmoid form.

Shoulders (2000) speculates that he might be observing the fundamental mechanism by which the vacuum can manifest charge creation. The EVO typically manifests a charge of 100 billion electrons and contains about 100,000 ions. It manifests a charge to mass ratio (e/m) the same as the electron. The ratio appeared even when Shoulders created positive EVO (a rare event), and this event proved that the EVO was not a simple collection of electrons (or positrons) because when the positive EVO decayed, it did not manifest 0.5 MEV gamma rays characteristic of electron-positron annihilation. Another unusual characteristic is that when on a dielectric, the EVO can sometimes stop emitting light and go dark. He has named these entities "black EVO," and he can excite them back into the visible, light-emitting state with a small voltage pulse.

It was the detailed study of the boreholes in aluminum oxide that convinced Shoulders the EVO hold their energy in a coherent form, not as heat. The sloshing characteristic of the melt from the borehole implied that the EVO captured and entrained the liquid ceramic. It was as if the EVO directly disrupted the ceramic's atomic bonds to produce the liquid melt, and the unscarred ceramic next to the borehole showed that heat could not be the cause of the melt. This observation seems similar to the Brown's gas welding behavior.

Perhaps the biggest anomaly associated with EVO phenomena is transmutation of elements. Shoulders (2004) analyzed the material in the crater of EVO strikes and discovered new elements that were neither in the cathode emitter or anode target material. Moreover, the new elements had unusual isotopic content not readily found in

nature. Shoulders is not alone in this discovery. The Proton-21 Laboratory in the Ukraine (Adamenko, 2004) has conducted super nucleo-synthesis experiments where they strike very pure copper or tungsten targets with large plasmoids (~1 cm diameter), and likewise observe the creation of multiple new elements of unusual isotopic content. So far these results have been ignored by academia in the United States, but they are continuously studied in Russia (RCCNT&BL-16, 2009). If these experiments could be replicated and confirmed in the U.S., the possibility for a new technology to alter and remediate radioactive waste might arise.

Ken Shoulders offers an easy protocol for generating a plasmoid like phenomena the manifests unusual energetic anomalies. He is willing to help any university seeking to replicate his research.

REFERENCES

Adamenko, S. V., "Results of experiments of collective nuclear reactions in superdense substances," Proton-21 Electrodynamics Laboratory, Lyiv, Ukraine, (2004).

Allan, S. D., "HybridTech releasing water fuel generator plans," pesn.com, (2009).

Allan, S. D., "OS: Self-Looped Anton HHO Cell System" peswiki.com, (2010).

Allan, S. D., "Claim: Running a Truck on Water" peswiki.com, (2010 b).

Beene, J., "Scam or no?" mail-archive.com, (2007).

Bostick, W. H., "Experimental Study of Plasmoids," *Phys. Rev.*, **106**(3), 404 (1957), [also; "Plasmoids," *Scientific American*, **197**, October, (1957), p 87].

Brown, Y., "Welding," U.S. Patent 4,014,777, (1977).

Celenza, L. S., Mishra, V.K., Shakin, C.M. and Liu, K.F., "Exotic States in QED," *Phys. Rev. Lett*, **57**(1), 55 (1986).

Chambers, S. B., "Apparatus for Producing Orthohydrogen and/or Parahydrogen," U.S. Patent 6,126,794 (2000), [also; U.S. Patents 6,419,815 (2002) and 6,790,324 (2004)].

Cole, D. C. and Puthoff, H. E., "Extracting energy and heat from the vacuum," *Phys. Rev. E*, **48**, (1993), pp. 1562-1565.

Couch, C. M., "Company runs truck on 100% hydroxy," pesn.com (2010).

Davis, E. W., Teofilo,V. L., Haisch, B., Puthoff, H. E., Nickisch, L. J., Rueda, A. and Cole, D. C., "Review of Experimental Concepts for Studying the Quantum Vacuum Field," in the proceedings of *Space Technology and Applications International Forum* (STAIF 2006), edited by M.S. El-Genk, AIP **CP813**, (2006), pp 1390-1401.

Eckman, C., "Plasma Orbital Expansion of the Electrons in Water," *Proceedings of the Natural Philosophy Alliance*, (2010), pp 141-144. (Reprint)

Gamow, G., *Thirty Years that Shook Physics*, Doubleday, NY, (1966).

Hasslberger, S., "Ken Shoulders' EVOs – Exotic Vacuum Objects Challenge Particle Theory" blog.hasslberger.com (2007).

Jennison, R. C., "A New Classical Relativistic Model of the Electron," *Phys. Lett. A*, **141**(8/9), (1989), pp 347-382.

Kelly, P., *A Practical Guide to Free Energy Devices*, Automotive Systems, (2008), Chapter 10, (Reprint).

King, M. B., *Tapping the Zero-Point Energy*, Adventures Unlimited Press, Kempton, IL, (1989).

King, M. B., *Quest for Zero-Point Energy*, Adventures Unlimited Press, Kempton, IL, (2001).

Kuhn, T. S., *The Structure of Scientific Revolutions*, University of Chicago Press, Chicago, (1970).

Laughlin, R. B., *A Different Universe: Reinventing Physics from the Bottom Down*, Basic Books, NY, (2005).

Neumark, D., "Hydrated Electrons Can Take More Than One Guise," *Research News Berkeley Lab*, December, (2004).

Ohmasa, R., "Ohmasa Gas by Japan Techno Co., Ltd.," Peswiki.com, (2009).

Panacea, "Hydroxy Course," panaceauniversity.org, (2010).

Prevenslik, T.V., "Bubbles and Steam Electricity," *ESD Journal*, (2001).

Prigogine, I. and Nicolis, G., *Self-Organization in Nonequilibrium Systems*, Wiley, NY, (1977).

Prigogine, I. and Stengers, I, *Order Out of Chaos*, Bantam Books, NY, (1984).

RCCNT&BL-16, "The 16th Russian Conference on Cold Nuclear Transmutation and Ball-Lightning" iscmns.org, (2009).

Scheck, F., *Leptons, Hadrons, and Nuclei*, North Holland Physics Publ., NY, (1983), pp 212-223.

Senitzky, I.R., "Radiation-Reaction and Vacuum Field Effects in Heisenberg-Picture Quantum Electrodynamics," *Phys. Rev. Lett.*, **31**(15), (1973), p. 955.

Ravi, R., "Research Paper on Ravi's Water Fuel Cell Replication," panaceauniversity.org, (2008).

Shea, J., "HHO Games," hhogames.com, (2008).

Shoulders, K. R., "Energy Conversion Using High Charge Density," U.S. Patent 5,018,180, (1991).

Shoulders, K. R., "Permittivity Transitions" svn.net, (2000).

Shoulders, K.R., "Low Voltage Nuclear Transmutation" svn.net, (2004).

Sokol, J.D., "You Can Turn Water Into Fire," turnwaterintofire.com, (2009), [The e-book no longer contains Steven Eaton's electrolyzer plans.]

Suartt, T. and Gourley, R., "Method for Making a Gas from an Aqueous Fluid, Product of the Method, and Apparatus Therefore," International Publication Number: WO 2008/131126 A1, wateriontechnologies.com, (2008).

Turtur, C. W., "The Fundamental Principle of the Conversion of Zero-Point Energy of the Vacuum," philica.com, (2010).

Watanabe, M., Misono, N., Osanai, Y., Shiina, S. and Saito, K., "Self-organization and dynamo responses in toroidal confinement plasmas," in the proceedings of *XXVII International Conference on Phenomena in Ionized Gases,* Topic number 14., the Netherlands, (2005), ([Reprint](#))

Wheeler, J. A., *Geometrodynamics*, Academic Press, NY, (1962).

Windisch, S., "[Brown's Gas (HHO): "Clean, Cheap and Suppressed Energy](#)," peswiki.com, (2008).

Wiseman, G., "[Eagle Research: Brown's Gas](#)," eagle-research.com, (1998).

Wiseman, G., "[News Flash: New evidence of the unique properties of Brown's gas](#)," eagle-research.com, (1999).

Wiseman, G., "[The Best Brown's Gas Technology in the World](#)," watertorch.com, (2001).

Wiseman, G., "[Brown's Gas Water Torch Research & Applications – Lecture](#)," youtube.com, (2007).

The Flow of Energy

Frank Znidarsic[1] and Glen A. Robertson[2]

[1]*Registered Professional Engineer in the state of Pennsylvania*
Johnstown, PA 15906
814-535-5302; fznidarsic@aol.com

[2]*Institute for Advanced Studies in the Space, Propulsion & Energy Sciences*
265 Ita Ann, Madison, AL 35757
256-694-7941; gar@ias-spes.org

Abstract. In this paper, the flow of energy in materials is presented as mechanical waves with a distinct velocity or speed of transition. This speed of transition came about through the observations of cold fusion experiments, *i.e.*, Low Energy Nuclear Reactions (LENR) and superconductor gravity experiments, both assumed speculative by mainstream science. In consideration of superconductor junctions, the LENR experiments have a similar speed of transition, which seems to imply that the reactions in the LENR experiment are discrete quantized reactions (energy - burst vs. continuous). Here an attempt is made to quantify this new condition as it applies to electrons; toward the progression of quantized energy flows (discrete energy burst) as a new source of clean energy and force mechanisms (*i.e*, propulsion).

INTRODUCTION

Mechanical waves are a local oscillation of material, where 1) Only the energy propagates, 2) The oscillating material does not move far from its initial equilibrium position, and 3) The wave travels by jumping from one particle of the medium to another. Therefore, mechanical waves transport energy and not material. However, a mechanical wave requires an initial energy input to be created. But once the initial energy is added, the wave will travel through the medium until all the energy has been transferred.

Recent observation of the speed of transition (a measure of the flow of energy) within speculative experiments seems to indicate a mechanical wave within the atomic nucleus that is discrete or quantized. This leads to the proposal of a new quantum condition, where Planck's constant emerges as a condition on the speed of the electronic wave within the electronic structure of the atom. Whereby, the speed of a transverse electronic wave equals the speed of a longitudinal mechanical wave within the nuclear structure.

However for new phenomena to occur, the energy procuring the mechanical wave needs to be discrete (quantum) burst versa a (classical) continuous emission, thereof. Whereby, the high energy flow must occur in one burst, without bounce, and without destroying the system. This paper is an attempt to quantify this new quantum condition as it applies generally to electrons.

NEW OBSERVATIONAL SPEED OF MECHANICAL WAVES

Two experiments seem to have similarities in their speed of transition; the Low Energy Nuclear Reactions (LENR) (Kitamura *et al.*, 2009) and superconductor gravity experiments (Podkletnov and Nieminen, 1992; Podkletnov and Modanese, 2003), both assumed speculative by mainstream science. The LENR experiment is discussed in the

following to establish the equation for the speed of transition followed by a brief mentioning on the superconductor gravity experiments with an analysis given later in the paper.

Low Energy Nuclear Reactions

Thermal energy, nuclear transmutations (to include transmutation of heavy elements), and a few high energy particles have reportedly been produced during cold fusion experiments, *i.e.*, Low Energy Nuclear Reactions (LENR), to include the reported transmutation of heavy elements (Miley and Patterson, 1997). According to contemporary theory (Lawson, 1957), heavy element transmutations can only progress at energies in the millions of electron volts. However, the available energy at room temperature is only a fraction of an electron volt. Whereby, these experimental results do not fit within the confine of the contemporary theoretical constructs; *being widely criticized on this basis*. Further, LENR experiments (Mosier-Boss *et al*., 2007) have produced very little, if no, radiation; another source of contention. However it is suggested that nuclear reactions can proceed without producing radiation under a condition where the range of the nuclear spin-orbit force is extends through the coulombic barrier. Whereby, the process of cold fusion may require a radical restructuring of the range and strength of the natural forces. The condition of the active nuclear enviroment provides some clues.

Low level nuclear reactions proceed in the domain of the reactions $r_N \sim 50 \ nm \ \left(i.e., \ 5 \times 10^{-8} m\right)$, where there is a positive thermal coefficient of frequency f_N or angular frequency $\omega_N = 2\pi f_N \sim 10^{13}$ to $10^{14} \ Hz$. The product $\omega_N r_N \equiv 2\pi f_N \times r_N$ then implies a speed V_t of transition on the order of $\sim 10^6 \ m/s$. That is, a transitional speed

$$V_t = \left(\frac{2\pi f_c}{n_i}\right) n_x r_x \Rightarrow \left(\frac{n_x}{n_i}\right)\left(\frac{2\pi \cdot r_x}{\lambda_i}\right) c \tag{1}$$

with the thermal frequency f_N expressed as a fraction n_i of the Compton frequency $f_c = c/\lambda_i$. Noting that for $f_c = 1.236 \times 10^{20} \ Hz$ and $r_x = r_e/2 \approx r_N$ with $n_x = n_i$, the speed of transition $V_t \approx 1.0942 \times 10^6 \ m/s$.

Equation (1) then defines the speed of the mechanical wave within the dissolved deuterium of the low level nuclear reactions with respect to discrete distances $n_x r_x$ and particle wavelengths $n_i \lambda_i$, where with $r_x = r_N \sim 5 \times 10^{-8} m$ the ratio n_x/n_i is of the order of 10^{-24}; indicating that $n_i \gg n_x$ in these nuclear reactions.

> In classical mechanic, $V_t \to c$, such that, $n_x r_x \to \frac{1}{2\pi} n_i \lambda_i$ or $n_x \approx n_i$. That is, classically the reaction range r_x is defined by a given material and the wavelength λ_i by the particle in motion through the material. Here it is postulated that when the particle wavelength $n_i \lambda_i$ becomes discrete (quantized), so must the reaction range $n_x r_x$. Whereby, energy flow also becomes discrete (quantized), *i.e.*, energy burst vs. continuous flow, which could produce higher energy flow for brief periods than normally seen in classical systems; leading to new phenomenon of study.

Superconductor Analogy

For example, superconductors are discrete (quantized) electron systems. Superconductor Josephson junctions or layers existed on order of a few $nm \equiv r_J \sim 10^{-9} m$. Robertson (2011) indications that the superconductor electron pair fluctuation time is $\sim 10^{14} s$, which implies (under normal conditions) a maximum electron angular frequency $\omega_e \sim 10^{14} \ Hz$ or electron fluctuation frequency $2\pi f_e \sim 10^{14} \ Hz$. Whereby, the product $\omega_e r_J \equiv r_J \times 2\pi f_e$ implies a speed V_t of transition (*i.e.*, the separation speed required to release the electron pairing energy in order to cross the junction) on the order of $\sim 10^6 \ m/s$.

Further, Li and Torr (1992) and Torr and Li (1993) published calculations of the propagation behavior of gravitational waves inside a superconductor (SC). They claimed that the phase velocity of gravitational waves in any

SC material would be $\sim 10^6\,m/s$. That is, the speed of gravitational energy through the superconductor is the transitional speed as defined by equation (1).

Superconductor Gravitational Anomaly

In the early 1990's, a team lead by Podkletnov (Podkletnov and Nieminen, 1992; Podkletnov and Modanese, 2003) using a two layer high T_c superconducting disk, reportedly produced a strong gravitational anomaly, which does not appear to fit within the contemporary scientific construct – *the generation of a strong local gravitational field seems to violate the conservation laws*.

Summary

The similarity in the speed of transition to the superconductor <u>would seem to imply that the reactions (energy burst) in the LENR experiments were discrete and on the order of electron pairing energy</u>. Further, the implications of the two speculative (LENR & Gravity Anomaly) experiments appear to place a minimum velocity *with respect to distance and time* from which "free" energy (*i.e.*, vacuum energy, dark energy or etc.) can be pulled from the subatomic scale ($\sim 10^{-9}\,m$) interactions. This new understandings of the progression of an energy flow may lead to new sources of clean energy and force mechanisms (*i.e*, propulsion).

THE SPEED OF A MECHANICAL WAVE WITHIN THE NUCLEUS

Potential energy is given as

$$E = \frac{1}{2} K_e \left(2r_x\right)^2 . \tag{2}$$

By letting the electron elastic constant K_e emerge from the maximum electron force $F_{max} \approx 29.1\,N$ between the redistribution of electrons at an average distance r_x being of close proximity to the nucleus, it is can become discrete and given as

$$K_e = \frac{F_{max}}{n_x r_x} , \tag{3}$$

where in classical systems $n_x = 1$.

Now by noting that, the electron elastic constant K_e equals that of the strong nuclear force at points where the expansive electromagnetic force balances the compressive strong nuclear force and expelling the electrical force to the circumference of the nucleus, the discrete speed V_t of transition becomes a product of the frequency of a harmonic oscillator and a displacement, *i.e*,

$$V_t = \frac{n_i \lambda_i}{2\pi} \sqrt{\frac{K_i}{m_i}} , \tag{4}$$

where i indicates a given particle of mass m_i and wavelength $\lambda_i \approx r_i \sqrt{2}$ [in classical systems $n_i = 1$].

For classical neutron with mass $m_n \approx 1.6749 \times 10^{-27}\,kg$, radius $r_i = r_x = r_n \approx 1.36\ x\ 10^{-15}\,m$ and $n_i = n_x = n_n = 1$, then equations (3) and (4) can be combined to yield speed of a mechanical wave within the nucleus as

$$V_t = \frac{1}{2\pi} \sqrt{\frac{F_{max}}{2r_n} \times \frac{1}{m_n}} \times 2r_n \approx 1.0932 \times 10^6\,m/s ; \tag{5}$$

a product of the harmonic motion of the neutrons at a displacement equal to the Fermi spacing $\approx r_n$ [the neutrons radius].

ELECTRON SPEED OF TRANSITION

Equations (1) and (5) imply that the energy in an atom emerges as a classical affect of a condition where the speed of light within the electronic structure of the atom equals the speed of a mechanical wave within its nuclear structure, where the equalization of velocities aligns the impedance of the interacting states. This impedance match allows energy to be exchanged, without reflection, and the quantum transition to progress.

Modes of differing impedance are evanescent and block the flow of energy. Such that, from the photo-electric effect, the speed of quantum transition of an emitted photon of frequency f_i can be given as

$$V_t \approx f_i \lambda_i, \tag{6}$$

where the energy of a photon emerges from the interaction on the transitional wavelength λ_i to produce an electrical charge of wavelength λ_e. The simultaneous emergence of both the photon's frequency and electron energy is fundamental to Bohr's principle of complementarity; reconciling the duality of particles and waves.

When dealing with electron potential energy, capacitance must first be defined as a function of the geometry. By letting the area swept out by a light wave equal to its wavelength squared and setting the distance between the peaks in the wave's amplitude equal to one half wavelength, the capacitance experienced by such a cycle of light is given as

$$C = \frac{e_o \lambda_e^2}{\frac{1}{2}\lambda_e}. \tag{7}$$

The reduction of equation (7) expresses the geometry of the transitional quantum state in terms of its electrical capacitance as

$$C = 2e_o \lambda_e. \tag{8}$$

Combining equations (6) and (8) expresses the capacitance of the transitional quantum state in terms of its frequency as

$$C = 2e_o \left(\frac{V_t}{f_e} \right). \tag{9}$$

The energy of electron charges is expressed in terms of its capacitance as

$$E = \frac{1}{2}\left(\frac{Q^2}{C} \right), \tag{10}$$

which when combined with equation (9) gives the photo-electric energy as

$$E = \left(\frac{Q^2}{4e_o} \right)\left(\frac{f_e}{V_t} \right). \tag{11}$$

Now since the photoelectric energy relationship to the electric charge is give by

$$E = hf_e = 2\pi\hbar \cdot f_e; \tag{12}$$

whereby, combing equations (11) and (12) gives photo-electric speed of transition

$$V_t = \frac{Q^2}{4e_o h} = \frac{Q^2}{8\pi e_o \hbar} = 1.0938 \times 10^6 \ m/s \tag{13}$$

for a single charge $Q = e = 1.60 \times 10^{-19} C$; showing that the Planck constant $\hbar$ emerges as a condition on the speed of transition of electrons in a bulk mass.

ELECTRON ORBITAL RADIUS

It is proposed here that the quantum structure of the atom is established at points of energetic accessibility. These points, of matching impedance, are qualified by setting the speed V_t of a mechanical wave in the nuclear environment equal to *the speed of light within the electronic structure*; were

$$V_t = \omega_e r_{or} \approx \omega_e n_x r_B .$$

(14)

where $r_B \approx 5.29 \times 10^{-11} m$ is the bohr radius. That is, the product of the electron's angular frequency ω_e and its orbital radius $r_{or} \approx n_x r_B$.

Now by letting $\lambda_e \approx \pi r_e$ and $n_i = n_e$, the electron speed of transition can be given from equation (4) as

$$V_t = \frac{n_e r_e}{2} \sqrt{\frac{K_e}{m_e}} .$$

(15)

Combining equations (3) and (15) then gives the speed of transition as

$$V_t = \frac{n_e r_e}{2} \sqrt{\frac{F_{max}}{n_x r_B} \times \frac{1}{m_e}} = 1.0938 \times 10^6 \ m/s .$$

(16)

where the value infers the classical speed of transition with $n_x = n_e = 1$. Equation (16) then yields

$$r_{or} \approx n_B r_B = \frac{F_{max}}{M_{-e}} \left(\frac{n_e r_p}{V_t} \right)^2 = n_e^2 \times \frac{F_{max}}{M_{-e}} \left(\frac{r_p}{V_t} \right)^2 \approx n_e^2 \times r_{+h} .$$

(17)

As it was then noticed that

$$\frac{F_{max}}{M_{-e}} \left(\frac{r_p}{V_t} \right)^2 \approx 5.29 \times 10^{-11} m \approx r_{+h} ,$$

(18)

where r_{+h} is the ground state radius of the hydrogen atom. Whereby, the electron orbital radius r_{or} is a square multiple of the number n_e of electrons times the ground state radius r_{+h} of the hydrogen atom.

THE CLASSICAL DEBROGLIE WAVE AND THE TRANSITIONAL FREQUENCY

De Broglie (1924) suggested that the matter wave naturally emerges, from the superposition of the Compton wave and its Doppler shifted refection, given by

$$f(t) = sin\left(2\pi f_c t + \pi \right) + sin\left(2\pi f_c \left(1 \pm \frac{v}{c} \right) t \right) .$$

(19)

Here we let

$$2\pi f_c t + \pi = 2\pi f_c t \left(1 \pm \frac{v}{c} \right)$$

(20)

and replace the Compton frequency with its contemporary value of the Compton frequency to yield

$$\left(\frac{m_i c^2}{\hbar}\right) t + \pi = \left(\frac{m_i c^2}{\hbar}\right) t \left(1 \pm \frac{v_i}{c}\right), \tag{21}$$

where v_i is the particulate mass velocity. Equation (21) can be further deduced to yield

$$ct = \pm \frac{\pi \hbar}{m_i v_i}. \tag{22}$$

This result implies that the deBroglie wave of matter be given as

$$\lambda_d = \frac{2\pi\hbar}{m_i v_i}. \tag{23}$$

Combining equation (23) with equation (6) yields the speed of transition as

$$V_t = 2\pi\hbar \left(\frac{f_i}{m_i v_i}\right). \tag{24}$$

Equation (24) specifically applies for the electrons of mass $m_i = m_e$, such that, when the mechanical wave equals the electronic wave, the particulate velocity v_i is equal to the photo-electric speed of transition, equation (13). Combining equations (13) and (24) for the electron, where $Q = e$ and $f_i = f_e$, then gives

$$V_t = \left(\frac{4\pi\hbar}{e}\right)^2 \left(\frac{e_o}{m_e}\right) f_e, \tag{25}$$

where equation (25) can be applied to any electron transitional state and establishes the baseline frequency needed to obtain the transition speed, where

$$f_e = \left(\frac{m_e}{e_o}\right) \left(\frac{e}{4\pi\hbar}\right)^2 V_t, \tag{26}$$

Which for $V_t \approx 1.0938 \times 10^6 \, m/s$, $f_e = 1.6448 \times 10^{15} \, Hz$, which is of the range of the LENR, but about twice that of the gravitational anomaly experiments.

Superconductor Analogy

For the electron pair ($n_e = 2$), the frequency the transitional speed $V_t \approx \omega_{2e} r_x \equiv (f_e/n_e) \times r_x$. Combining this with equations (25), yields

$$r_J \approx 2 \left(\frac{4\pi\hbar}{e}\right)^2 \left(\frac{e_o}{m_e}\right); \tag{27}$$

the junction spacing required for a transition speed of $V_t \sim 10^6 \, m/s$. Then for $e = 3.2 \times 10^{-19} \, C$, $\hbar = 1.05457 \times 10^{-34} \, J \cdot s$, $e_0 = 8.85 \times 10^{-12} \, A \cdot s / V \cdot m$ and m_e=9.11×10^{-31} kg, equation (27) yields $r_x \approx 1.3300 \times 10^{-9}$ m, which is the ballpark estimate for the Josephson junction gap distance in superconductors, *i.e.*, the range of range of electron pair energy transition.

CONCLUSION

The concept of a speed of transition was presented. Indications are that at speeds of transitions at or greater than $\sim 10^6 \, m/s$ new phenomena can occur. The similarity in the speed of transition between the speculative Low Energy Nuclear Reactions (LENR) and Gravity Anomaly experiments appear to place a minimum velocity *with respect to*

distance and time from which "free" energy (*i.e.*, vacuum energy, dark energy or etc.) can be pulled from the subatomic scale ($\sim 10^{-9} m$) interactions. This new understandings of the progression of an energy flow may lead to new sources of clean energy and force mechanisms (*i.e*, propulsion).

NOMENCLATURE

r_e = 2.818 x 10^{-15} (the classical radius of the electron (meters))

f_c = 1.236 x 10^{20} (the Compton frequency (Hertz))

F_{max} = 29.05 (the electrical charge force maximum (Newtons))

m_e = 9.109 x 10^{-31} (the mass of the electron (kg))

r_{+h} = 0.529 x 10^{-10} (the radius of the hydrogen atom (meters))

r_n = 1.36 x 10^{-15} (the nuclear Fermi spacing (meters))

V_t = 1.094 x 10^6 (the transitional velocity (meters/second))

REFERENCES

de Broglie, L., *Recherches sur la théorie des quanta* (Researches on the quantum theory), Thesis, Paris, (1924).

Kitamura, A., Nohmi, T., Sasaki, Y., Takahashi, A., Seto, R. and Fujita, Y., "Anomalous Effects in Charging of Pd Powders With High Density Hydrogen Isotopes," *Physics Letters A*, **373**(35), (2009), pp. 3109-3112.

Lawson, J. D., "Some Criteria for a Power Producing Thermonuclear Reactor," *Proceedings of the Physical Society B*, **70**, (1957), p. 6.

Li, Ning and Torr, D.G., "*Gravitational effects on the Magnetic Attenuation of Superconductors*," *Physical Review B*, **46**(9), (1992).

Mosier-Boss, Szpak S., Gorden F. E. and Forsley L. P. G., "Use of CR-39 in Pd/D co-deposition Experiments," *European Journal of Applied Physics*, **40**, (2007), 293-303.

Podkletnov E. and Nieminen, R., "A Possibility of Gravitational Force Shielding by Bulk YBa2Cu307-x Superconductor," *Physica C*, vol 203, (1992), pp 441-444.

Podkletnov, E. and Modanese, G., "Investigation of High Voltage Discharges in Low Pressure Gases through Large Ceramic Superconducting Electrodes," *Journal of Low Temperature Physics,* **132**(3/4), 3 (2003).

Modarres, M., "Momentum Distributions of Nuclear Matter," *Europhys. Lett.* **3**, (1987), 1083.

Miley, G. and Patterson, J. A., "Nuclear transmutations in thin-flim nickel coatings undergoing electrolysis," *J. of New Energy*, (1997), pp. 5-30.

Mosier-Boss, P. A., Szpak, S., Gordon, F. E. and Forsley, L.P.G., "Use of CR-39 in Pd/D co-deposition experiments," *Eur. Phys. J. Appl. Phys*., **40**, (2007), pp. 293-303.

Robertson, G. A., "Quantum Effects in the Type II Superconductor that Lead to Power Radiated in Gravitational Waves," to be in the ebook *Gravity-Superconductors Interaction: Theory and Experiment 2010*, Bentham e-books, Bentham Science Publishers, (to be released in 2011).

Torr, D.G. and Li, N., "Gravitoelectric-Electric Coupling via Superconductivity," *Found. Phys. Letts.* **6**, (1993), pp. 371-383.

A Hyper-Efficient Inverter Driven By Positive EMF In Combination With Transient Phenomenon

Osamu Ide

Clean Energy Research Laboratory
3-4-21-601 Mita, Minato-ku, Tokyo, Japan
03-5442-4746; office@yamatrans.co.jp

Abstract. In these days, quite a many types of electrical device/ unit use inverters as their key components. And, most of such inverters conventionally employ the Royer's circuit which is designed to use pulse current of rectangular form as input. On the other hand, the inverter prototype that the author has developed features the two points that 1) it employs pulse current of sharp spike form as input, and that 2) it takes advantage of transient phenomenon to be occurred simultaneously in the circuit for attaining a certain level improvement of the efficiency. Taking advantage of the above two features in combination; it becomes possible to develop a new type of inverter driven by positive EMF which gives outstanding efficiency. Now, consider what is "positive EMF"? It is electromotive force which is in the same direction as that of the input current. On the other hand, the so-called "back EMF" to be induced according to the well-known Faraday's law, is in the direction reverse to the input current. They are utterly different in nature. The value of the positive EMF to be induced in the coil depends on the rate of change of magnetic flux, where the second-order and even higher-order time derivatives of magnetic flux are involved.

INTRODUCTION

The fundamental working principles of the inverter by this invention are based upon the hypotheses and conclusions which were reported previously by the author (Ide, 1995; 2000). Therefore, before going into the detailed explanation on the inverter, the outlines of these references are described below.

In the earlier time before being involved in the research on this inverter, the author had been engaged for years in the research of an unusual phenomenon which is observed in association with electromagnetic induction. The outcomes from the research works made during these years, are the above-mentioned two research reports which are listed as the references cited in this research report. In brief, one of the important conclusions of the above two reports in combination, is that there is a possibility for "unknown electromagnetic induction" to exist in reality. And its property is far different from that of the electromagnetic induction in accordance with the Faraday's law.

In Ide (1995), the unknown EMF which is experimentally identified, is called as "positive EMF". The word "positive" means that the EMF to be caused is in the same direction as that of the input current. In other word, its direction is just reverse to that of the well-known "back EMF" to be induced according to the Faraday's law. The unknown EMF was discovered when the author was working in a series of experiments on a motor that introduces unique driving method.

In the earlier stage of the research, the author made investigation on the working characteristics of a type of motor to be driven by the current discharged from the capacitor to a pair of the coils of the stators. And, its rotor is located at the middle point between the two coils of the stator, and the axes of the two coils facing each other, are set in a common line.

In the result of the above investigation, it was discovered that an unusual type of EMF had been induced there, in the condition that the stator's two coils which are installed so as to face each other, are set in the repelling mode. In other word, such a phenomenon was observed only when two identical magnetic fields which were generated from each coil, repel each other. It is also discovered that difference between the experimentally observed value of EMF and the theoretical value calculated according to Faraday's law in the repelling mode. There is the difference of 3V between the both values.

In order to effectively explain the above stated phenomenon, the author proposed a hypothesis that "Only when electromagnetic fields generated constitute a special configuration, positive EMF may be caused". Here the word "positive" means its direction is in reverse to that of Faraday's "back EMF". When positive EMF is caused in a coil, the current in the coil will be accelerated, so that the intensity of the current will also be increased accordingly. Namely, current value in the coil will become much more than theoretically expected for an input voltage. In addition, as a by-product of the research, it has also experimentally been confirmed that the internal resistance loss of each coil, has been apparently reduced under the existence of such positive EMF.

In Ide (2000), a series of tests in the same experimental condition as that reported in Ide (1995), was conducted by using the identical motor whose coils of the stator are in a different design from that of the motor reported in Ide (1995). What is to be additionally noted there is that a new means was introduced to improve the precision of theoretical calculation for simulation to a further extent. The one more thing to be noted is the introduction of an "unusualness checking index". The index is represented as the deviation of experimentally observed value from theoretically calculated value.

In Ide (1995), it is reported that positive EMF is observed only in a pair of coils of the stators, which generate a pair of identical counter electromagnetic fields to repel each other. However, one of the conclusions reported previously by the author (Ide, 2000), suggests that positive EMF can generally appear in a coil of any type, design or condition, even though the effective EMF may not be strong enough, compared to those caused in the repelling mode.

In other words, it is possible for positive EMF to be caused more or less even in a common or ordinary electromagnetic system such as electric motor, electric generator and power transformer, although it may not be strong enough to be sensed by an ordinary measuring device. The reason for that is presumed to be that since such a common system uses input power of a low frequency sine wave form, the output level of caused positive EMF cannot be large enough. Even if someone else happens to experimentally discover such EMF in an usual electromagnetic system, the unusual data is very likely to be ignored or treated as a measurement error, because no such notion as "positive EMF" has been popular in the world of this day.

The other important conclusion reported previously by the author (Ide, 2000), is that there is orderliness in the data of caused positive EMF. The reason this discovery of such orderliness is largely owing to a drastic improvement in the precision level of simulation. In the result, a clear orderliness is recognized in the obtained deviation data. Here, deviation means the difference between the experimentally observed value and theoretical value calculated based the Faraday's law. Accordingly, if "positive EMF" exists in reality, it is natural to presume that the component(s) attributable to the positive EMF must compose the above said deviation. Based upon such consideration, the author has proposed a hypothesis that "positive EMF is a function of the second or higher time derivatives of the magnetic flux caused".

The well-known Faraday's EMF is expressed as the function only of the term of the first time-derivative of magnetic flux. Due to the fact that the second and/or higher time derivative components of magnetic flux have never been paid attention, even if someone found the phenomenon so far. it must have been ignored until today. There are two most important points be noted here, the first one is that the terms to reflect such non-linear components which are completely independent of the component of Faraday's EMF, exist in reality, and the second one that the direction of the non-linear components to act, are just in reverse to that of Faraday's EMF.

The working principle of the inverter by this invention totally reflects the cores of the hypotheses and conclusions obtained through the research works, which are described in the said two references. It is presumed that sharp spike pulse is more likely to cause positive EMF, because its steepness could effectively cause components of time-derivatives of the second and/or higher orders. If current of pulse of such a form is put to the input terminal of the primary coil of a transformer, actually due to the effect of positive EMF, the existing input current will be intensified

to a level which is further higher than that expected for an ordinary type of input power source. Consequently, it is possible to say that magnetic energy in the amount to exceed the value estimated from calculation may be caused within the transformer. This is one of the key points for developing a hyper-efficient inverter that is the theme of this research report.

HYPER-EFFICIENT INVERTER

As the readers already may know, an inverter is a unit to convert DC input power to AC output power. An inverter is basically composed of a transformer and an oscillating circuit to chop a DC input current. In most cases, the Royer's circuit is employed as the oscillating circuit. However, on the other hand, there is the most basic circuit such as shown in Figure 1, which uses a conventional method to produce AC power output in the secondary coil of the transformer, by simply repeating on-off switching actions onto the input current running in the primary coil. In the case of the inverter discussed here, the latter type circuit is adopted.
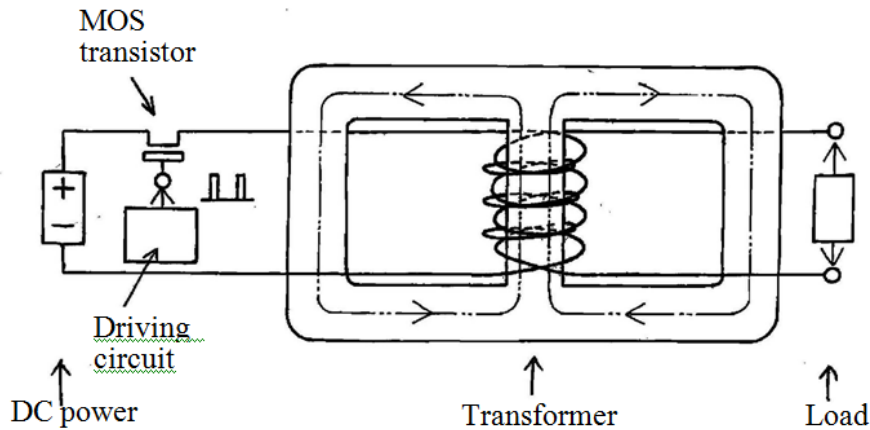
Figure 1. Schematic diagram of the inverter.

According to Faraday's law, output voltage from the secondary coil of a transformer, is determined only by the first order time-derivative of magnetic flux. When the inductance of the transformer is set to a constant value, output voltage from the transformer, is determined by the first order time-derivative of input current. (See the 1st term of the equation (1) shown below.)

$$EMF = \frac{d\Phi}{dt} = \frac{d(L \cdot i)}{dt} = L \cdot \frac{di}{dt} + i \cdot \frac{dL}{dt} , \qquad (1)$$

where, Φ is the magnetic flux, L is the inductance, i is the current, and t is time.

Therefore, input current which is mostly composed of DC component, is most disadvantageous for producing high AC voltage output. From such consideration, it is obvious that the Royer's circuit which is driven by current of approximately rectangular wave which is mostly composed of DC component, is inefficient.

The ideal wave form of driving pulse current in order to extremely reduce DC component, is a spike form. It makes it possible to minimize time for DC current to flow in the primary coil of a transformer. However, it is practically difficult for us to produce driving pulse current of such a form. To overcome the problem, the author introduced triangle pulse wave as an alternative of it, which has an advantage in feasibility.

Based on the above consideration, we developed a unit to generate steep triangle form pulse wave by employing a switching circuit composed of MOS transistors. In the case of this, it is practically unavoidable to have the non-steep area at the summit of each triangle composed of the two sides (the rise-up side and the fall-down side). See Figure 2.

Here the author temporarily calls thus generated "triangle form pulse" as "spike form pulse" because the author thinks that we should regard the former as the practical alternative of the latter, to proceed discussion conveniently at least in the remaining part of this report.

<div align="center">

(a)   (b)
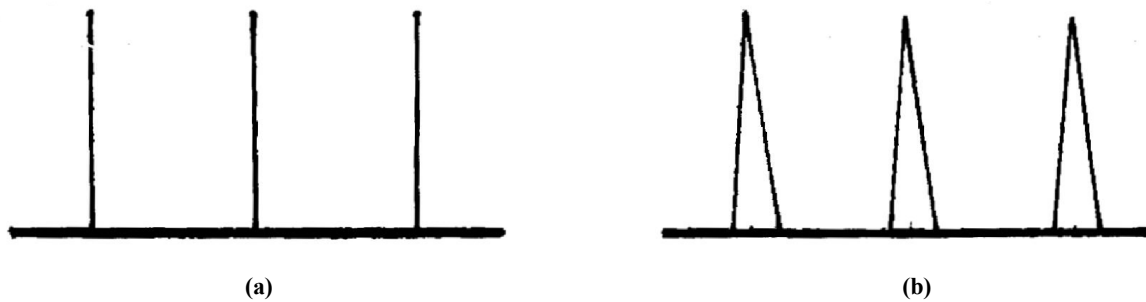
Figure 2. (a) Spike form pulse and (b) Triangle form pulse

</div>

Now, it is considered that the rise-up and fall-down sides of a spike form pulse, are made of very high frequency components. It is presumed that such a tendency is much more remarkable in the narrow but non-flat area at the summit of the triangle. Therefore, if pulse current of this type is input to the primary coil of a transformer, very sudden and sharp change will occur in the magnetic field of the magnetic core. That is, it is the very ideal condition to efficiently cause positive EMF induction. Because of that, spike form pulse current are used in the driving circuit of the inverter.

On the other hand, based on the results obtained in the references #1 ans #2, the author determined to integrate a special type of transformer which is designed to produce a unique electromagnetic configuration in the inverter. It is a method to generate positive EMF as well, on the other hand. In other word, it is a method to take advantage of a unique electromagnetic configuration to be created by a pair of counter magnetic fields repelling each other, which is located in the area of an air gap made in the transformer.

The above decision finally contributed to the successful development of a kind of hyper-efficient inverter. It has been examined that the inverter which has been developed thus , really has a high efficiency to always exceed that of any type of inverter existing.

Apart from the above, the author also succeeded in the development of another type of hyper-efficient inverter to use a common type of transformer as its basic component, with the introduction of a kind of innovative driving method. The detailed description of the by-product inverter is as follows.

After the first spike pulse is put in the primary coil of the transformer, the induced voltage corresponding, due to the transient phenomenon, will be caused in the secondary coil. Then in a timing before the induced voltage still remains in the secondary coil, the second spike pulse of the input current will be put in the primary coil. And the same action shall be made also for the third pulse and the subsequent pulses. By continuing such actions, current in the primary coil will be dramatically intensified in proportionate to the number of repetition. In the result, an avalanche-like phenomenon will occur, in which output voltage reaches an extraordinary high level.

It may be needless to say, but it should be noted that such a phenomenon occurs even in the condition that the secondary coil bears a resistor load. The level of the output voltage from the secondary coil, will saturate at a certain level depending on the value of the existing load. However, the level may reach more than double that of current simply caused by a single spike pulse.

It is possible to make the above stated phenomenon to happen by shortening the repetition interval of spike form pulses. The author calls this phenomenon as "avalanche effect". It can be caused by superposing a number of transient waves existing in the secondary coil. Owing very much to the avalanche effect, a hyper-efficient inverter, which is the target of this research, has been realized.

The electrical circuit diagrams of the prototype units, and the measurement results

Figure 3 shows the circuit diagrams of an inverter according to this invention, and its external appearance, where Figure 3(a) shows the electrical circuit diagram of the inverter in which a typical ordinary transformer is integrated, Figure 3(b) shows the electrical circuit diagram of the inverter in which a transformer according to this invention to generate a pair of counter magnetic fields to repel each other, is integrated, and Figure 3(c) shows the external appearance of the total system of the inverter used for experiments.
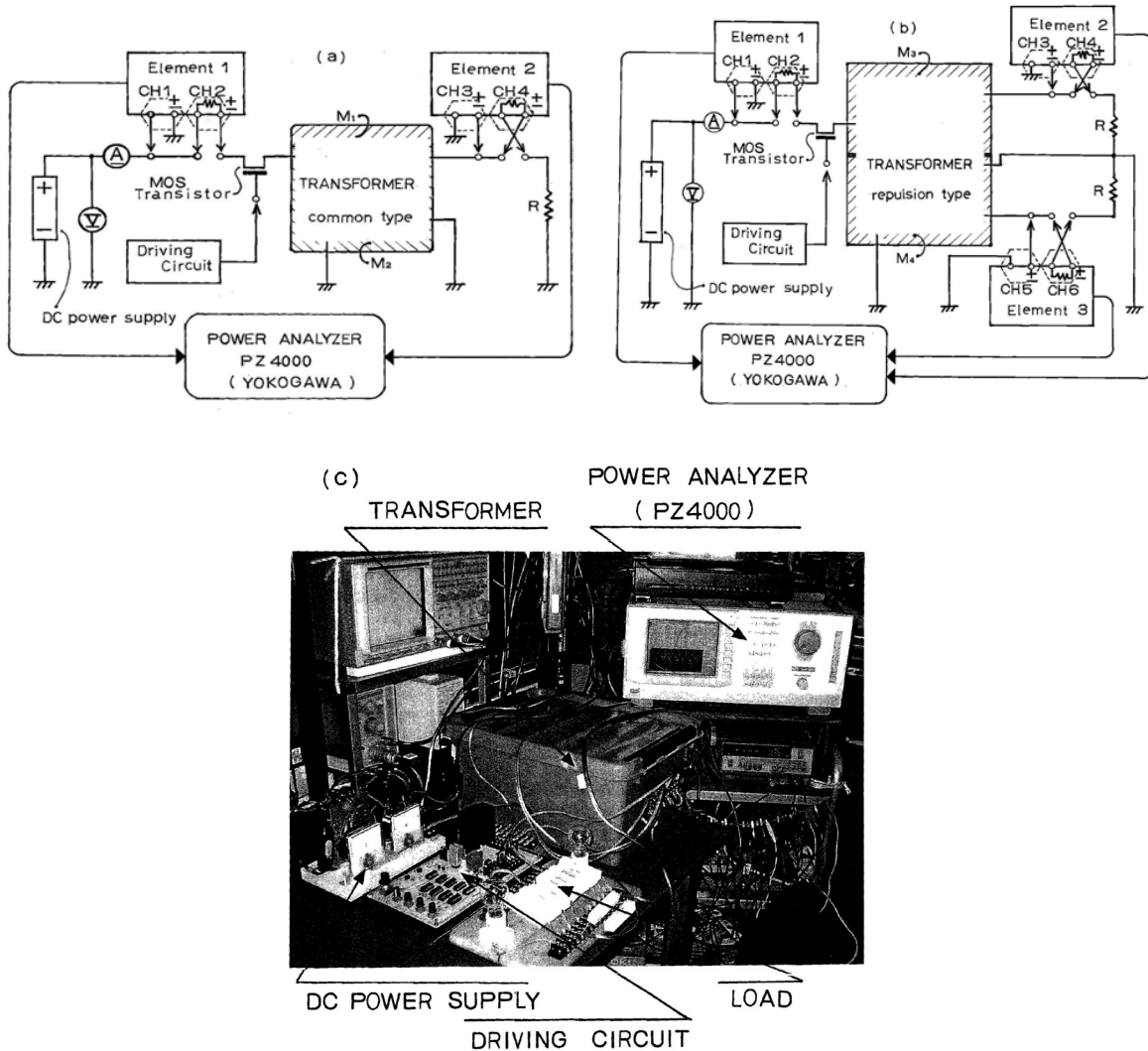
Figure 3. (a) Ordinary type of transfermer design, (b) Transformer design to produce counter magnetic fields, and (c) Experimental system.

In Figure 3 (a), direct current supplied from the DC power source whose voltage level is in the range of 38V to 54V, is input to the primary coil of the transformer after being chopped by a MOS transistor. The power to be output from the secondary coil of the transformer, is consumed in the load resistor R.

In Figure 3(b), a transformer which is designed so as to generate a pair of counter magnetic fields to repel each other, has two output terminals, to each of which a load resistance is connected.

M1, M2, M3 and M4, are magnetic cores of the coils, and has the same specifications. It is designed so that currents running in M3 and M4, shall build up a pair of counter magnetic fields to repel each other. It also should be noted that a thin air gap exists between the magnetic cores M3 and M4.

Measurement of the values of input power and output power to and from the inverter, was made by using Yokogawa's Power Analyzer PZ4000 shown in Figure 3(c). It is a four-channel unit featuring a high-speed sampling function. It has the capability to record the measured power values in parallel through the four channels, utilizing a number of voltage sensors and current sensors, each of which is electrically insulated from each other. Therefore, the device is able not only to calculate power, but also to show on the display unit, the digital values measured together with the wave forms, by each channel. It means that we could get the correct value of RMS even in the case in which the obtained wave form is distorted or crooked to a certain extent. Moreover, from data of wave forms stored in the memory, it is also possible to calculate the value of RMS of voltage, current and/or power in any desired time span.

Element 1, Element 2 and Element 3 in Figure 3, are power sensor units. Element 1 is one for input, and Element 2 and Element 3 are ones for output. Incidentally, in the case of a transformer to generate a pair of counter magnetic fields to repel each other, the value of the output power will become equal to the sum of those of Element 2 and Element 3.

CH1, CH3 and CH5 are the voltage sensors. Each of them has input impedance of 1 mega ohms, and electrically insulated [floated] from the others. CH2, CH4 and CH6 are the current sensors. Each of them has the shunt resistance of 0.1 ohm, and is electrically insulated from the others. The sampling frequency is 5 mega Hertz, and the vertical resolution is 12 bits.

For the purpose of confirmation, measurement of output values from the DC power source was made by using other type of measuring devices, and compared to those obtained by using the Power Analyzer PZ4000. In the result, it is found that there is no significant difference between the two cases, although it is recognized that the data obtained from the Power Analyzer PZ4000, tends to be slightly larger. .
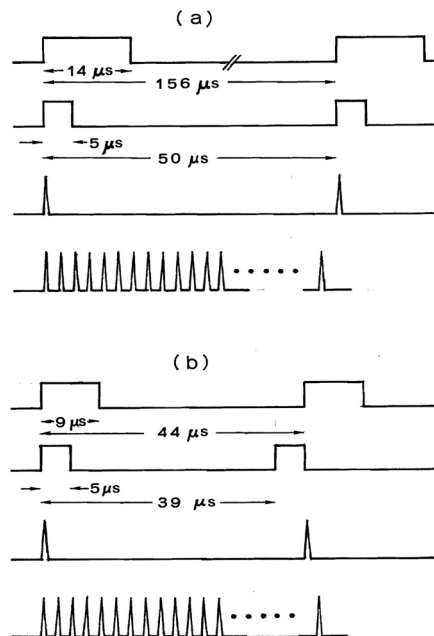
Figure 4. The wave forms of the driving pulse current used in the transformer of an inverter by this invention: (a) Wave form used in an ordinary transformer; (b) Wave form used in a transformer designed to produce   counter magnetic fields
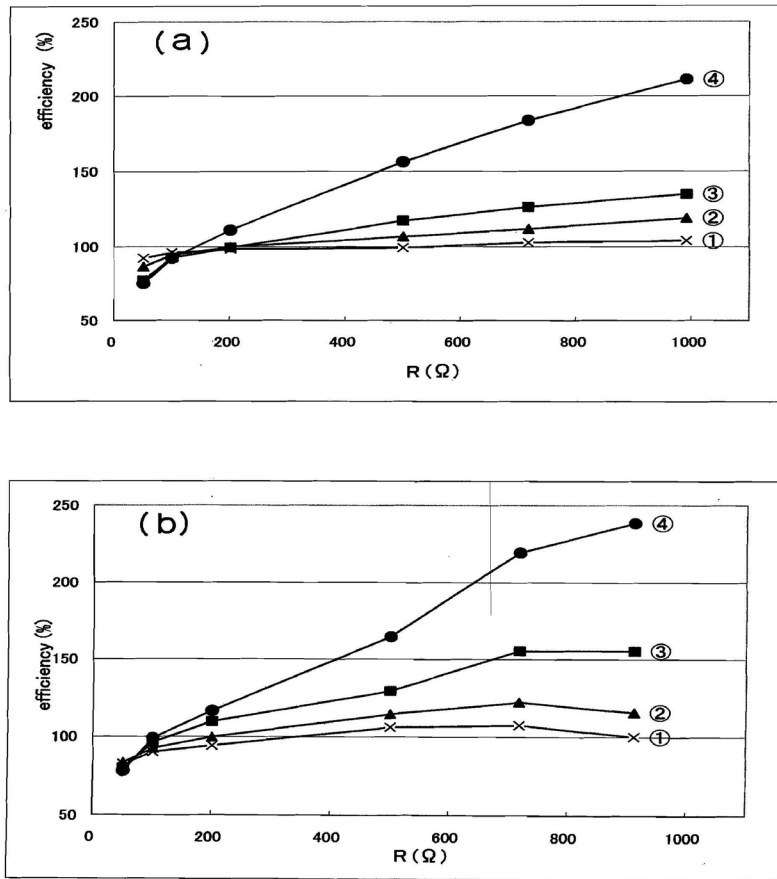
Figure 5. The relations of efficiency (%) and load resistance (ohm) of the inverters tested: (a) Inverter having an ordinary transformer; (b) Inverter having a transformer designed to produce counter magnetic fields

The electrical circuits of the system, which is employed in the prototype units used for the experiment, was driven using a number of types of driving pulse signal (parameters), for the purpose to check the differences. Figure 4 shows their wave forms. Namely, Figure 4(a) is the typical wave forms of the driving pulse used for an ordinary transformer, which corresponds to the circuit diagram shown in Figure 3(a). Figure 4(b) is the wave forms of the driving pulse used for a transformer according to this invention, which corresponds to the circuit diagram shown in Figure 3(b). (The latter transformer is designed so as to build up a pair of counter magnetic fields to repel each other.)

In Figure 4 (a) and Figure 4 (b), <1> is a square shape pulse wave with a larger DC component, <2> is the square wave of a smaller pulse width, <3> is a spike wave whose DC component is at a minimum, and <4> is so called "quick pulse wave" whose repetition cycle is shorter than of <3>.

Figure 5 shows the results of the measurements. The x-axis is load resistance, and y- axis is the efficiency (%) of the inverter. <1>, <2>, <3> and <4> shown in Figure 5, correspond to <1>, <2>, <3> and <4> shown in Figure 4, respectively.

The curves in Figure 5(a) show the result of the measurement on an ordinary transformer, and the curves in Figure 5(b) shows the result of the measurement on a transformer according to this invention, which is designed to generate a pair of counter magnetic fields to repel each other.

Each point indicated in the curves, is the average value calculated from as many as 400 to 8000 wave forms obtained in a series of experiments.

ANALYSIS OF THE RESULTS AND CONSIDERATIONS

This section discusses the results of an analysis of the inverter and considerations of the design. To accomplish this, this section is divided into three sections covering the advantages of the characteristics of spike waves, the transformer design and an inverter to make quick spike pulses.

Inverter to take advantage of the characteristics of spike wave pulse

From the result shown in Figure 5, it is known that with the introduction of spike form as the driving pulse wave form, the efficiency of either an ordinary transformer or a transformer according to this invention, could be improved to a great extent.

From the wave forms shown in <1>, <2> and <3> of Figure 4, it is also known that the more the driving pulse wave form becomes likely to spike wave form, the higher the efficiency will become.
The wave form <1> shown in Figure 5(a) that has the largest DC component, corresponds to the condition that is most close to the case of an ordinary inverter. It is beyond anticipation that it still has the efficiency in the level to slightly exceed 100% even in such condition.

Here, the author would like to make consideration on the above phenomenon, based upon the wave forms recorded in the Power Analyzer.

Figure 6 shows the wave forms of output voltage, recorded in the Power Analyzer PZ4000, in the case that input voltage to an ordinary transformer is driven by a single square pulse wave having a large DC component. Figure 6(a) shows a single square wave pulse to drive input voltage to the transformer. Figure 6(b) shows the output voltage wave form in the case that the load resistance is small (R=50 ohms). Figure 6(c) shows the output voltage wave form in the case that the load resistance is large (R=991 ohms).

Incidentally, because the load is composed only of ohm resistance(s), the output current wave form becomes likely to the output voltage wave form. Numerical values (%) shown in Figure 6(b) and Figure 6(c) are the efficiencies of each divided section of the wave form.

Speaking of Figure 6(b) for example, the efficiency of the section in the range from the point when input current starts to run, to the point when it is turned off, is 84%. The efficiency of a short period immediately after input current is turned off, is 196%. The efficiency of one single cycle of square wave driving pulse, is 87%. These values happen to coincide with the average of hundreds of the values which are obtained from the wave form analysis. See Figure 5(a).

 In contrast to the above, as for the section of the wave form shown in Figure 6(c), during a certain period immediately after input current starts to run, a high level of efficiency of 142% is observed. In the time period after the moment until input current is turned off, the efficiency is 85%.

Thereafter even after the value of input current becomes close to zero, remaining transient waves of voltage to run in the reverse direction, continues to exist. The efficiency in this time period is still kept in a high level to exceed 100%.

The total efficiency in a single cycle of square wave pulse, is calculated based on the above results, as 103%. This value coincides with that shown in Figure 5(a).

There are two important points to be noted on the data shown in Figure 6. The first point is the fact that a higher efficiency has been obtained particularly in the area which is ordinarily regarded as noise generated when the switch of input current is turned on or off. The second point is the fact that even after input current decreases to the level of near zero, the transient wave remaining in the secondary coil of the transformer continues to exist for a longer time than expected, while the efficiency of the transformer in this duration is in a fairly higher level as well.

The section to give the lowest efficiency of 84% or 85%, exists near the middle point of the driving pulse width where the value of DC component becomes maximum. Interesting enough, these values are close to those in the case of an ordinary inverter. In the case its output is mostly used in the form of direct current after rectifying it.

(a)

(b) +V   0

84 %   196 %

87 %

(c) +V   0

142%→

85 %

103 %
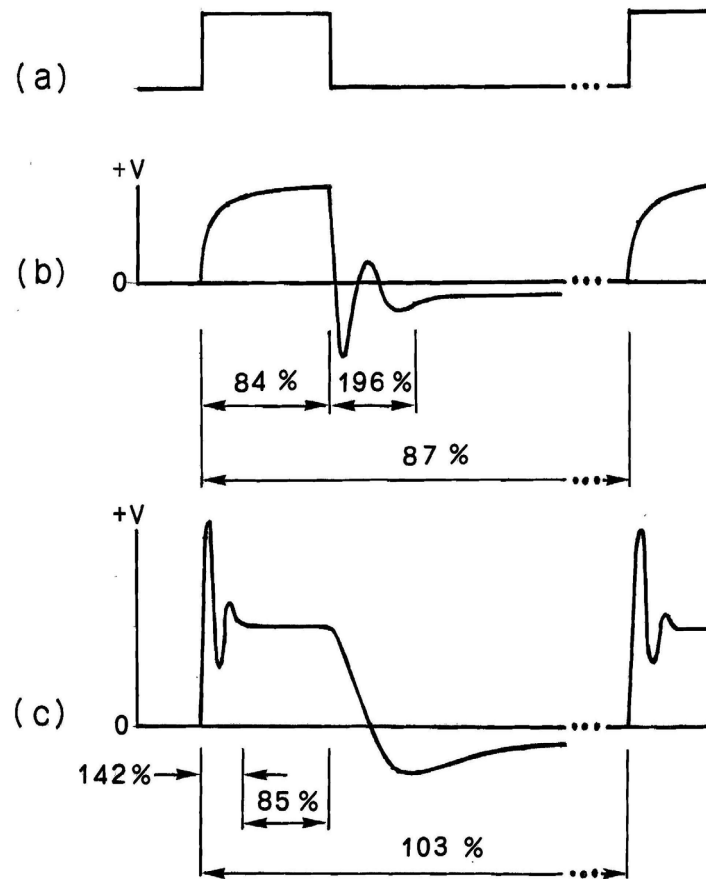
Figure 6. Output voltage's wave forms observed when an ordinary transformer is driven with a single square wave; (a) The driving pulse's wave form; (b) wave form of the case of small load resistance; (c) wave form of the case of large load resistance.

Oscillating waves of relatively large amplitude is caused when the input switch is turned on/off. Such waves have been treated as a cause of noise, and ignored so far. The phenomenon may be very much responsible for preventing an inverter of hyper efficiency from being developed before the inverter of this invention by this invention appears. On the other hand, the inverter by this invention, makes effective use not only of the most efficient portion which is caused by switching actions to turn on/off the input current, but also of the remaining transient waves to be caused after the switch is turned off, for generating output power. Particularly, by the introduction of spike wave pulse, it will become possible to make use only of the most efficient portion, if not including the flat DC component. It is presumed that the introduction of spike form pulse wave is the key factor to make successful the development of an inverter that produces a hyper efficiency of unexpected level.

In addition, based on the above facts, it is also presumed that positive EMF to be caused when the switch of input current of spike wave pulses is turned on/off, is the key factor to bring about such a hyper efficiency.

Transformer designed to make use of counter magnetic fields

One of the common conclusions reported in the both literature of the references #1 and #2 which are cited in this report, is that considerably strong positive EMF is observed of a motor which has a design to have a magnetic configuration having a pair of counter magnetic fields.

Here a pair of counter magnetic fields is magnetic fields to be generated from a pair of coils, having the identical magnetic polarity N or S, and being set in the geometrical position so as to face each other and to mutually repel, while sandwiching a thin air gap between them.

It is almost impossible to find in the market, a conventional type of transformer which is designed to give such a magnetic configuration.   The reason for that may be in that people think in that way "even if a set of coils having the design to produce counter magnetic fields repelling each other, is feasibly available, the original efficiency will be impaired to a great extent. It is a common sense". In addition, it is a commonly known fact that to install an air gap in the coils' cores, becomes the cause of the leak of magnetic flux, leading to lowering the efficiency of a transformer.

On the other hand, through the research activities made by the author so far, it has been discovered that it is very effective to install a component designed to produce a pair of counter magnetic fields in a transformer, for the improvement of its efficiency, by introducing a special method to drive the electrical circuit.

For example, if spike wave pulse current is input to a transformer having the circuit designed to generate a pair of counter magnetic fields, in the instance of a sharp rise-up, positive EMF will be caused to accelerate the current running in the pair of the coils facing each other to generate counter magnetic fields.

On the other hand, in the instance when the spike current is turned off, it will work so as to quickly decrease the current remaining in the coils. (Note: This phenomenon may also be explained by the Lentz's law.)

It is presumed that acceleration and deceleration of the current running in the primary coil, could act very effectively on the output of the secondary coil. In other words, in this case, it is speculated that during the transient time period to be caused when the input switch is turned off or on, a considerably larger magnetic energy is caused in such a transformer, than in the case of an transformer having an ordinary magnetic configuration which is shown in Figure 1, supposing that the amplitudes of each input voltage are same.

An additional improvement of the efficiency of an inverter has been attained by means to introduce a unique method to drive such a new type of transformer as above-mentioned. The method is to use spike wave form pulse, as input current. In comparison of the curve 5(a) of an ordinary transformer, to the curve 5(b) of a transformer having a design to produce counter magnetic fields, it is quite obvious that the latter exceeds the former in any aspect, supposing the characteristics of the driving wave are same.

Inverter to make use of quick spike pulses

If the first pulse of spike form pulse current is put in the primary coil of the inverter shown in Figure 7(a), voltage and current of the similar form will be caused in the secondary coil bearing a resistive load. However, the output voltage will widely change or oscillate along the amplitude axis from not only the positive value range but also the negative value range, and it will remain to exist for a fairly long time. Let us call this wave as "remaining transient wave".

If the second spike pulse (indicated by the arrow "A" shown in Figure 7(b)) is put in the primary coil before the transient wave which has been caused by the first spike pulse and is remaining in the secondary coil, disappears, a dramatic scale change in the magnetic flux will be caused, compared to that of the case in which the second spike pulse is input to the primary coil after the remaining transient wave has already disappeared. (Figure 7(a) and 7(b))

Particularly it is presumed that sudden change in the magnetic flux will be caused in the conditions that transient wave remaining in the secondary coil, runs in the reverse direction of that in the primary coil, and that the absolute value of the amplitude of the remaining transient wave is large enough.

On the other hand, it is also possible to make another consideration from a different angle. Namely, we can regard the above fact as that both the primary coil and the secondary coil of a transformer, will generate magnetic flux which are in a sort of repelling mode, as they are.

This view is backed up with the conclusions of the author (Ide, 1995; 2000) that two identical magnetic fields facing each other in the repelling mode will cause most strong positive EMF. Therefore, in the timing when the absolute value of positive EMF exceeds that of the Faraday's back EMF, the input current in the primary coil will start to be accelerated.

Namely, the positive EMF caused by the first pulse, will help intensify the second spike pulse, so that the intensity of the input current will virtually increase and exceed that due to the first spike pulse.

What is to be noted here is that the input current will increase in the condition that voltage level of the input DC power source is maintained at a constant value. In the result, the strength of the remaining transient wave which is caused in the secondary coil due to the second pulse will become quite large.

Then, when the third spike pulse is subsequently input in the primary coil in the timing before the remaining transient wave disappears, much stronger positive EMF will be caused. (Figure 7(c) and 7(d)).

If such actions as the above are made repeatedly, the output voltage will be increased in every repetition cycle, so that the phenomenon of avalanche-like amplification of output voltage will finally occur. However there exists a maximum limit of the level of the output voltage and its value will approach to a certain constant value of saturation in a short time. (Figure 7(e)).

The above stated avalanche-like phenomenon to be caused by the effect of superposition of remaining transient wave is one of the key features of an inverter by this invention. The phenomenon which will occur immediately after the power switch is turned ON can be visually observed using a measuring unit such as Power Analyzer PZ4000. But when repetition cycle of spike pulse current is too low (or the interval between spike pulses is too large), such an avalanche-like phenomenon will not occur.

Here, further consideration is made on input and output of the inverter below. As stated above, one of the key points on this inverter's working principle, is that spike form pulse current which is put in the primary coil, will be intensified by the positive EMF which has been caused by the previous pulse, so that magnetic energy in the transformer will be increased. If the input current is intensified, the input power is also increased.
However, from the fact that the voltage of a DC power source is constant, it is obvious that the input power will simply increase in proportionate to the value of input current.
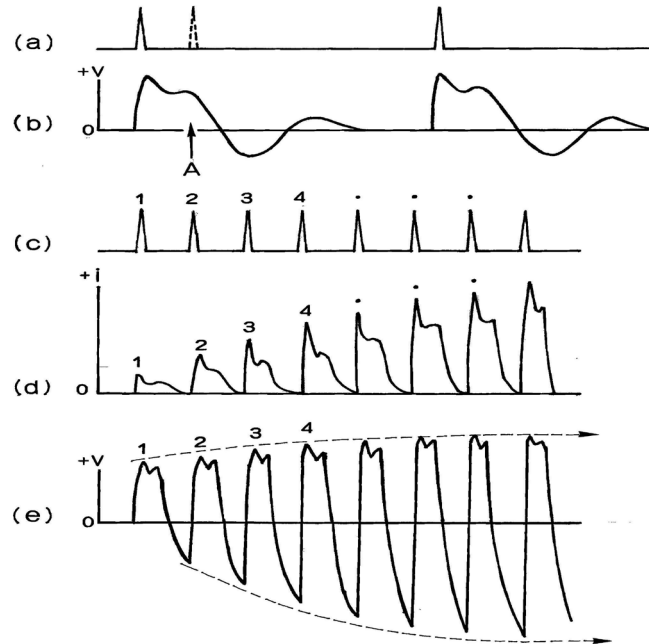Here, the author would like to ask the readers to pay attention to the following point. That is, the phenomenon of input current to be intensified, is not at all due to the length of time during which the switch of input pulse current is turned on. But, input current is intensified every time a spike pulse enters the primary coil during the time period of same length. That is caused by positive EMF which has been generated in the system. See Figure 7(c) and Figure 7(d).

Incidentally, in order to intensify input current in the coils of an ordinary transformer in which not such a phenomenon can occur, the only way to do so is to increase the driving time, in the conditions that output voltage of the DC power source, inductance of the coils and ohm resistance of each coil, remains constant.

On the other hand, the amount of magnetic energy held in a transformer, will increase in proportionate to the square of the input current. The magnetic energy is expressed by

$$E = \frac{1}{2} L \cdot i^2 \,, \tag{2}$$

where, L is the inductance of coil and i is the current.

Figure 7. Wave forms to show the avalanche effect observed when driving the transformer with quick spike pulses; (a) Wave of a single spike pulse to drive; (b) Waves of output voltage and current, caused by a single spike pulse; (c) Waves of quick spike pulse; (d) Waves of quick spike pulse current to be input to the transformer; (e) Waves of quick spike pulse voltage to be output from the transformer (an avalanche-like phenomenon).

The evidence to prove the above description can be obtained by observing the input/output wave forms of the inverter with Power Analyzer PZ4000. Namely, by the observation it is recognized that while the input power only increases in simply proportionate to the input current, both voltage and current of the secondary coil increase in proportionate to the strength of the input current. It means that the output power of the secondary coil has increased to a great extent. Therefore, it is concluded that the increasing rate of the output power will exceed that of input power.

According to the principle stated above, an improvement in the efficiency of an inverter has been attained successfully.

In addition, a total of seven test prototypes of inverter according to the specifications of the newly developed method, have been made so far. And, it has been confirmed that every one of them works properly as expected. In other words, there is no problem on the reproducibility of operation.

UNEXPLAINABLE PHENOMENA ON INVERTERS BY THIS INVENTION

The phenomena listed below are still unexplainable:

1. The values of output currents which are measured by using a 100 mega Hz digital storage oscilloscope (Panasonic VP-5740A) in combination with a clamp type current probe (Tektronix A6303, AM503), are always far larger than those recorded by Power Analyzer PZ4000.

2. Amount of heat generated from the load resistance which is connected to the output terminal of the transformer, is not large enough to meet the value expected from the corresponding output power value measured. In addition, it seems that the apparent load resistance has been decreased by a unknown reason.

3. No remarkable temperature rises in the inverter system, were not observed through a number of operations. On the contrary, it is observed in most cases that the temperature of part of the magnetic cores composing of the transformer is lowered to a level below the room temperature, or it sticks around the original temperature.

4. There is an index called "differential efficiency" to assess the efficiency of an inverter. The index is expressed by the ratio of the increment of output to the increment of input. If trying to calculate the index of an inverter according to this invention based on the measured data, the index value will be more than 1000%.

5. If the value of input power to the transformer is measured with the load resistances connected to the output terminals of the transformer, the RMS value of input power, will become negative when the load resistance value goes beyond the threshold value (singular point). It is known from a wave form analysis that this phenomenon is caused by the phase difference between input voltage wave and input current wave. Simply interpreting this phenomenon, the efficiency of a transformer as a single unit becomes infinite at the singular point, and its value will become negative in the range beyond the singular point, the value of the efficiency becomes negative. This fact means that the transformer is generating energy not only from the secondary coil to which the load resistances are connected, but also from the primary coil on the input side.

The author believes that each of the above mentioned items is interesting to the reader of this report, as well. These shall be the core themes of research in the coming future.

SUMMARY AND CONCLUSIONS

The author developed a new type of inverter which is composed of a unique driving circuit to be controlled by switching operation of the MOS transistors, and a transformer which is designed to produce unique magnetic configurations. And, a series of experimental tests to confirm the feasibility of the inverter were performed. The tests were made under the following conditions:

1) To use driving pulses of spike wave form, which have much less direct current components..
2) To use a transformer designed to produce a magnetic configuration composed of a pair of counter magnetic fields of the same polarity to repel each other
3) To use a special circuit driving method to amplify the output power of the transformer to a large extent, by means of shortening the repetition cycle of the spike wave pulse, and of superimposing the transient waves still remaining in the transformer's coils onto the lately input spike pulse.

In the result of a series of experiments, the following points are discovered:

#1 Efficiency of the tested inverters, is improved to a considerable extent, by introducing spike wave form pulse to drive the circuit, compared to the case in which square wave pulse having a DC component is used.
#2 Efficiency of the tested inverters, is much improved by introducing into the inverter system the magnetic configuration composed of a pair of counter magnetic fields to repel each other, compared to the case of an ordinary transformer.
#3 Efficiency of the tested inverters, is far more improved by using "quick spike wave" pulse having a shorter repetition cycle as the input current, instead of the normal spike wave pulse mentioned in #2, than in the case of #2
.

The author believes that the above discoveries can be explained based upon the hypothesis of "positive EMF" that has already been proposed in the references #1 and #2 of this report. However, the phenomenon that the efficiency of the tested inverters exceeds 100%, is still unexplainable.

ACKNOWLEDGEMENTS

Funabashi. The electrical connection diagrams of the system of the test units as well as of the Power Analyzer PZ4000, were checked for confirmation by Mr, Masatoshi Kono from Yokogawa Co. Ltd. English translation of the whole text of this report was made by Mr. Eiichi Yamamoto from Yama Trans Co, Ltd. The author is deeply grateful to the sincere efforts made by all of the above mentioned people, for this report to be completed successfully.

REFERENCES

Ide , O., "Increased voltage phenomenon in a resonance circuit of unconventional magnetic configuration," *J. Appl. Phys.*, **77**(11), (1995), pp. 6015-6020 (Preprint).

Ide, O., "Possibility of existence of non-linear electromotive force (EMF)," in the *Fifth International Symposium on Magnetic Suspension Technology*, edited by Nelson J. Groom and Colin P. Britcher, NASA/CP-2000-210291, (2000).

Increased voltage phenomenon in a resonance circuit of unconventional magnetic configuration

Osamu Ide

Clean Energy Laboratory, Natural Group Corporation, Shinagawa, Japan

The behavior of an *LCR* (inductance-capacitance-resistance) circuit with a movable ferromagnetic core is discussed. The core is attracted by a magnetic field generated by an electric current resulting from the discharge of a capacitor in the closed *LCR* circuit. An unusual increase in recharge voltage, which was dependent on the magnetic configuration of the coil, was observed. This voltage increase does not conform to the mathematical simulation of the system. The possibility that a positive electromotive force was involved in this effect is discussed. © *1995 American Institute of Physics.*

I. INTRODUCTION

The author has been developing a motor operated by the discharge of a capacitor in an *LCR* (inductance-capacitance-resistance) circuit. Unlike conventional dc motors, this motor utilizes the magnetic force of attraction between a current-carrying coil and a movable ferromagnetic core. The force of attraction between the two components resulting from the capacitor discharge is converted to a rotary force. The unconsumed magnetic energy is recycled as electrical energy by recharging the capacitor.

In the course of developing this motor, it was discovered that the recharge voltage depends on the precise configuration of the system.

The purpose of this paper is to describe the increased voltage phenomenon observed in the above system. A differential equation that expresses the phenomenon, as well as computer simulations, are also discussed.

It is appropriate here to briefly discuss other machines based on a similar magnetic phenomenon. Many attempts have been made to operate machinery that utilizes the nonlinear phenomenon of magnetism, such as ferroresonance[1,2] and parametric resonance.[3] The basic features of these machines is the magnetic saturation effect. The machines primarily make use of the transition from a nonresonant state to a resonant state, i.e., from the high inductance of a nonsaturated state to the low inductance of a saturated state, converting these two modes to either oscillation or amplification.

It should be noted that the present system is completely different from these machines, since there is no magnetic saturation in the coils. Voltage changes found in the system occur during the transition from a low-inductance state to a high-inductance state, and are not subjected to the sudden drop or rise typically associated with ferroresonance and parametric resonance. In other words, other systems operate in a closed magnetic field, whereas the system described here operates in an open magnetic field. Electrically, this system is basically closed, since the only power source used here is a charged capacitor; it has no ac power supply such as that used to operate other magnetic machines.

II. *LCR* CIRCUIT WITH AN INCREASE IN INDUCTANCE

The basis of the system discussed in the present paper is a conventional *LCR* circuit. Figure 1(a) shows a basic *LCR*

circuit containing a capacitor initially charged to a voltage of $+V_0$. When the circuit is closed, the capacitor discharges its energy through the inductor. The voltage and current in this transient state are known to follow a damped oscillation [Fig. 1(b)].

Switch S can be replaced by a SCR (silicon controlled rectifier) in order to eliminate switching loss [Fig. 2(a)]. The other advantage of using the SCR is that a negative charge in the capacitor is retained after discharge. The oscillation stops after the first discharge, since the SCR automatically turns off when the half-cycle current recharges capacitor C to a recharge voltage of $-V_r$. The voltage and current during this process are shown in Fig. 2(b). The amount of recharge voltage is always smaller than the initial voltage due to the resistance loss in the circuit.

The inductor (coil) in Fig. 2(a) is now replaced by two separate coils that face each other, with a movable ferromagnetic core inserted between the coils (Fig. 3). When the two coils (electromagnets) L_1 and L_2 are connected in series, they generate magnetic fields that attract the ferromagnetic core toward the coils.

Unlike when the core is fixed outside the coils (i.e., the core has no influence on the coils), the approach of the core results in an increase in combined inductance L, as well as movement of the magnetic flux near the coils. This increase in inductance and the movement of the flux naturally affect the discharge current and recharge voltage.

Generally speaking, it is expected that the total recharge voltage will decrease because this system produces mechanical output as the core moves. However, through a series of experiments, it was discovered that results depend on the magnetic configuration of the coils used in the circuit. In other words, for a certain kind of magnetic field, the opposite result could occur—an increase in the average current and recharge voltage. To confirm the above observations, an experiment was conducted, which is described in the following section.

III. INCREASED VOLTAGE PHENOMENON IN A *LCR* CIRCUIT

A. Experimental method

The experimental setup is schematically shown in Fig. 4. Ferromagnetic cores M_1 and M_2 are attracted to the rotor,
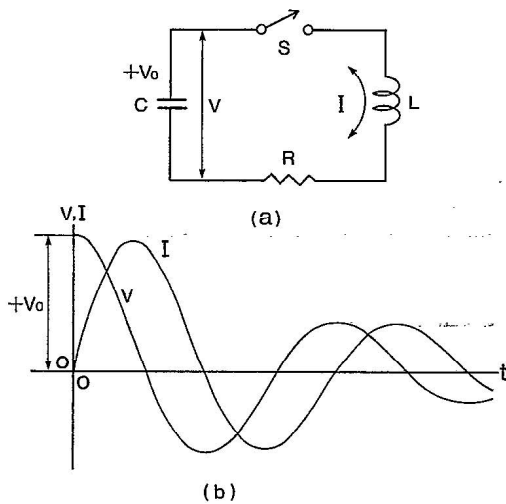
FIG. 1. (a) Basic *LCR* Circuit with a switch S. (b) Voltage and current oscillations of the circuit.

FIG. 3. *LCR* circuit with two coils and a movable ferromagnetic core inserted between the coils.

will vary slightly, depending on the direction of the magnetic fields. The reference point is exactly aligned with the electromagnets when the magnetic fields are attracting, and slightly displaced when they are opposing.

Figure 6 shows how the inductance of the electromagnet, measured by an *LCR* meter, is related to the displacement of

which is driven by a dc motor. The cores can be rotated at various speeds, with the speed of the axis being measured by a tachometer. Four electromagnets, L_1, L_2, L_3, and L_4 are connected in series and placed two-by-two in the stators facing each other. The number of turns, inductance (at 1 kHz), and dc inductance of the coils are, respectively, 169, 7.76 mH, and 1.22 Ω. The magnetic field of the electromagnets facing each other, L_1–L_3 and L_2–L_4, can either be attracting (i.e., N-S, N-S) or opposing (i.e., N-S, S-N). The former state will be called the "attracting mode" and the latter the "opposing mode." Placed between the two stators, each containing two electromagnets, is a rotor with two ferromagnetic cores. The specific positions of the electromagnets and the cores are schematically shown in Fig. 5.

At a certain distance between the coil and the core, combined inductance is maximized. This position of the core will be referred to as the "reference point." The reference point
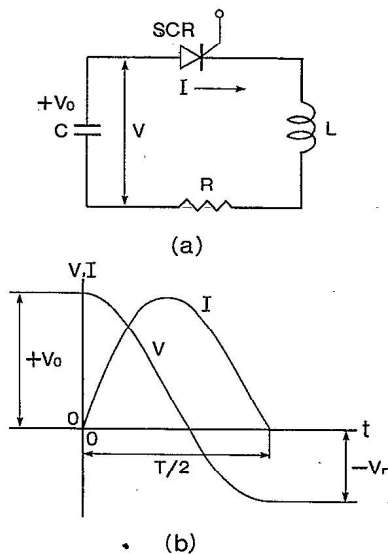

FIG. 4. Experimental setup.

FIG. 2. (a) *LCR* Circuit with a SCR instead of a switch. (b) Half-cycle voltage and current oscillations of the circuit.
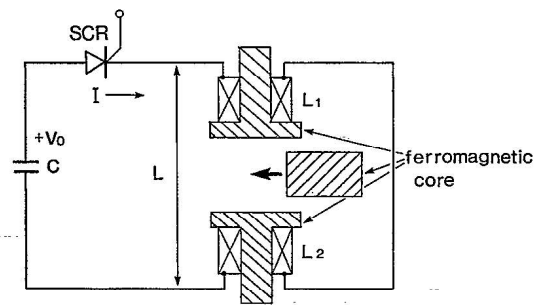
Osamu Ide

54
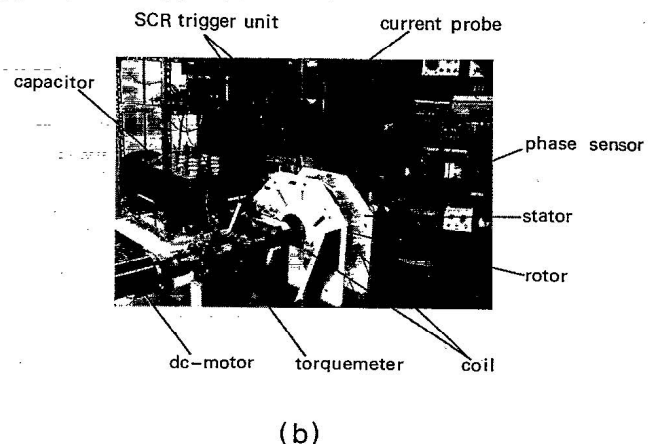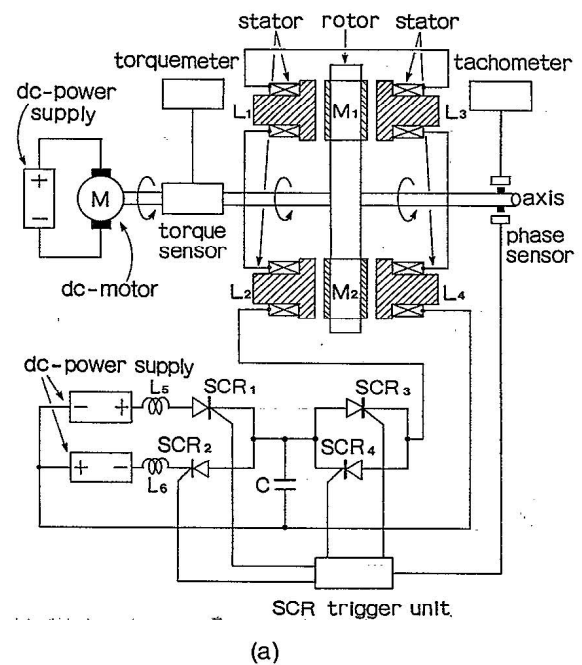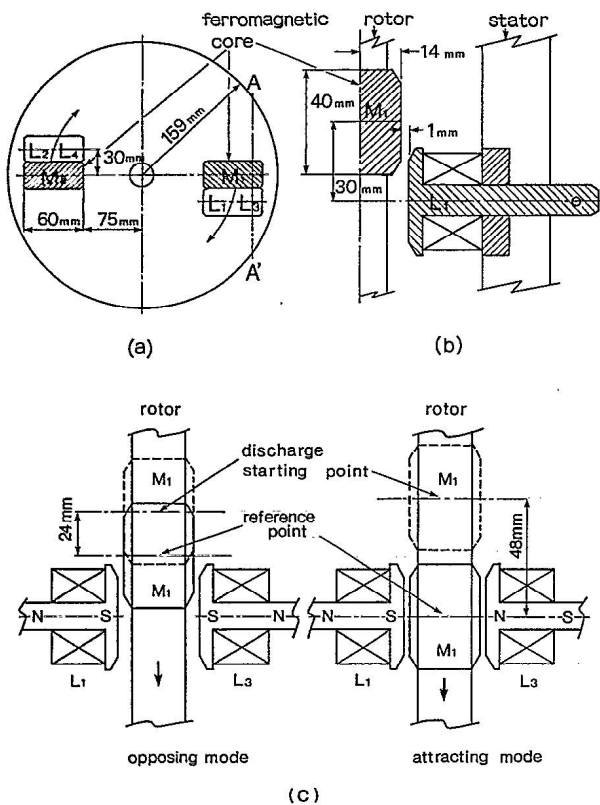
FIG. 5. Specific geometry of the electromagnets and the ferromagnetic core: (a) as viewed from the direction of the axis, (b) the cross section when cut from line A to A', and (c) the stator and rotor at the reference points and the discharge-initiation points.

the core from the electromagnet. The force of attraction (torque) between the electromagnet and the core is also indicated. This L-d (inductance-displacement) curve shows that the inductance gradually increases as the core approaches the magnet, reaching a maximum at the reference point ($d=0$). It can seen from the figure that the rate of change of inductance depends on the magnetic fields and is greater in the attracting mode.

A discharge is initiated at the distance from the reference point, at which the core can experience the maximum force
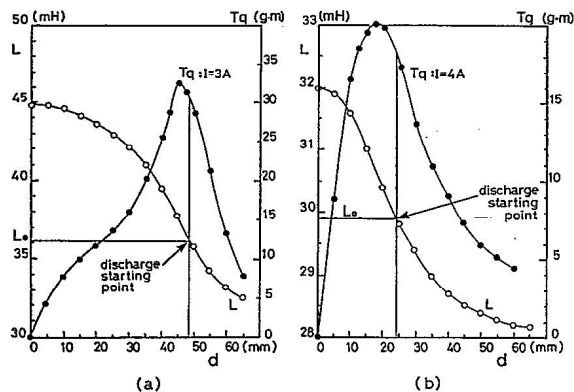

FIG. 6. Combined inductance (L) and torque (Tq) between the electromagnet and the ferromagnetic core. The torque was measured under conditions of constant current. Values of L and Tq for (a) the attracting mode, and (b) the opposing mode.
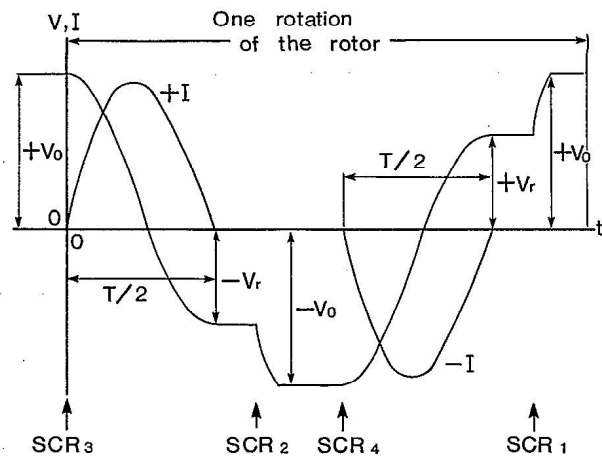

FIG. 7. Voltage and current changes during one rotation of the rotor. The SCR turn-on points are also indicated.

of attraction, i.e., $L=36.1$ mH in the attracting mode and $L=29.9$ mH in the opposing mode. The discharge is completed before the core reaches the reference point, indicating that the rotor does not receive a negative torque from the discharging coil.

The serial operation of the system (Fig. 7) is as follows:

(1) The capacitor is charged to $+V_0$.
(2) When the ferromagnetic cores approach the electromagnets, SCR 3 is turned on and the capacitor is recharged to $-V_r$.
(3) SCR 2 is then turned on and the capacitor is charged to $-V_0$.
(4) The same cycle is repeated with the opposite current by turning on SCR 4 and SCR 1 in succession (coils L_5 and L_6 are used for protection from an overcharge current).

Thus, for each half rotation, the positive and negative discharges are alternately repeated.

The positive and negative discharges are not completely symmetrical. The conditions for each discharge are not exactly the same due to the particular structure of the experimental device, such as the shape, size, and position of the core. This inevitably causes a slight difference in the recharge-voltage efficiency between two opposite discharges. This condition, however, applies to all cases examined.

Capacitance C is set at 15.87 μF, and the initial voltage V_0 at ±240 V. The capacitor voltage was measured by a high-voltage probe of 200 MΩ (dc~15 kHz) impedance, and the current was measured by a clamp-type probe. Wave forms of the capacitor voltage and the discharge current were simultaneously recorded using a digital-storage oscilloscope with a vertical resolution of 8 bits (1/256; the scale ranges from -320 to $+320$ V). Because of the dispersion of the data, eight measurements of the positive and negative discharges were recorded, and the averages were then examined. The estimated values was calculated by a computer connected directly to the oscilloscope.

B. Estimation factors

One estimation factor is the return-voltage rate, designated as **r**. This rate is defined according to the initial voltage V_0 and the recharge voltage $-V_r$ as

J. Appl. Phys., Vol. 77, No. 11, 1 June 1995

Osamu Ide   6017

55

$$\mathbf{r} = |V_r| / |V_0|. \tag{1}$$

Another factor is the apparent resistance R, derived from V_0, V_r, and current I. This value can be deduced using the following procedure. First, the energy relationship before ($t=0$) and after ($t=T/2$) the discharge is known as

$$E_0 = E_1 + E_r, \tag{2}$$

where E_0 is the initial electrostatic energy of the capacitor, E_1 the recharged electrostatic energy of the capacitor, and E_r the internal energy loss.

The values E_0, E_1, and E_r are expressed, respectively, as

$$E_0 = CV_0^2/2, \tag{3}$$

$$E_1 = CV_r^2/2, \tag{4}$$

and

$$E_r = R \int_0^{T/2} I^2 dt. \tag{5}$$

From these equations, R is written as

$$R = C(V_0^2 - V_r^2) \bigg/ \left(2 \int_0^{T/2} I^2 dt \right). \tag{6}$$

This value of R indicates not only the resistance measured in the dc current but also includes the eddy current loss and hysteresis loss, as well as the effect of back EMF (electromotive force). These resistances are generated when an inductor interacts with a ferromagnetic core. In short, R can be regarded as the total Joule loss of the inductor measured in the ac system.

As mentioned in the previous section, the voltage-current wave forms were accurately measured and recorded by a digital storage oscilloscope. From these waves forms, V_0, V_r, and ($\int I^2 dt$) can be calculated, and R can thus be estimated.

C. Results

Figures 8 and 9 show the results of the experiments. Return-voltage rate $\mathbf{r}$ and apparent resistance R are compared at different rotor speeds from near zero to 400 r/min.

When the magnetic field is in the attracting mode, the value of $\mathbf{r}$ follows a monotonic decreasing curve as the rotor speed increases. Correspondingly, resistance R follows an increasing curve. On the other hand, $\mathbf{r}$ is found to increase slightly in the opposing mode, with a peak in the 50–100 r/min range, and then gradually decrease at faster speeds. The values of R follow an opposite curve.

IV. MATHEMATICAL ANALYSIS

In order to fully understand the above phenomenon, a computer simulation of the relevant differential equation was made.

To describe the model, inductance L should be replaced by a time-dependent function $L(t)$ that expresses the serial change of L. It is clear that the combined inductance of the
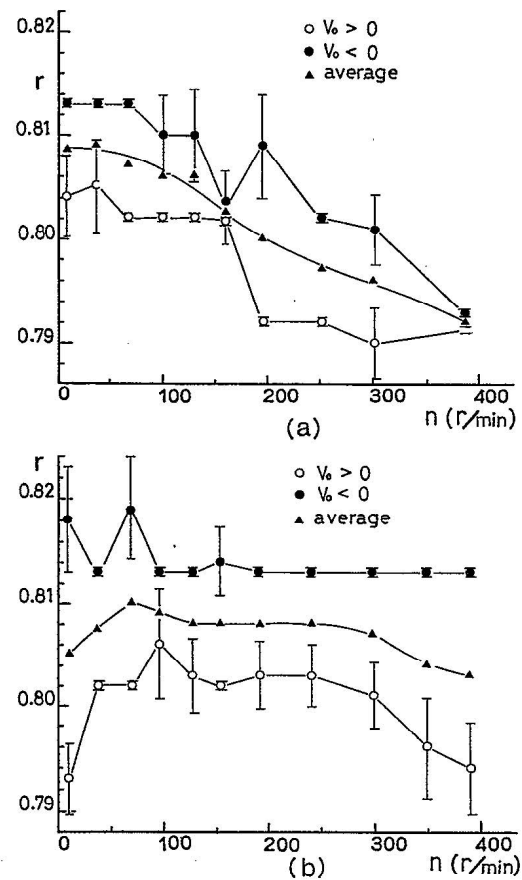
FIG. 8. Results of the experiment—voltage return rate ($\mathbf{r}$) for (a) the attracting mode, and (b) the opposing mode.

electromagnet and the ferromagnetic core is related to the speed at which the ferromagnetic core approaches the electromagnet.

In the experiment, discharge begins when the core experiences the maximum torque, with the core traveling only a very short distance. The change in inductance caused by this motion may be regarded as linear over this narrow range. Thus, the change in inductance can be expressed by the following equation:

$$L = L_0 + \alpha x \quad \text{(H)}, \tag{7}$$

where L_0 is the initial inductance of the electromagnet (H), α the rate of inductance change over the distance (H/m), and x the displacement of the core (m).

From $x = vt$, where v is the speed of the core and t is the duration of discharge, Eq. (7) can be transformed as follows:

$$L = L_0 + \alpha vt \quad \text{(H)}. \tag{8}$$

The value $\alpha v\,(\text{H s}^{-1})$ in this equation is the rate of inductance change over time. Since α is constant (unique to each coil), this rate is proportional to v.

From Faraday's law, the voltage across coil V_1 under conditions of changing inductance $L(t)$, is expressed as

6018   J. Appl. Phys., Vol. 77, No. 11, 1 June 1995

Osamu Ide

56
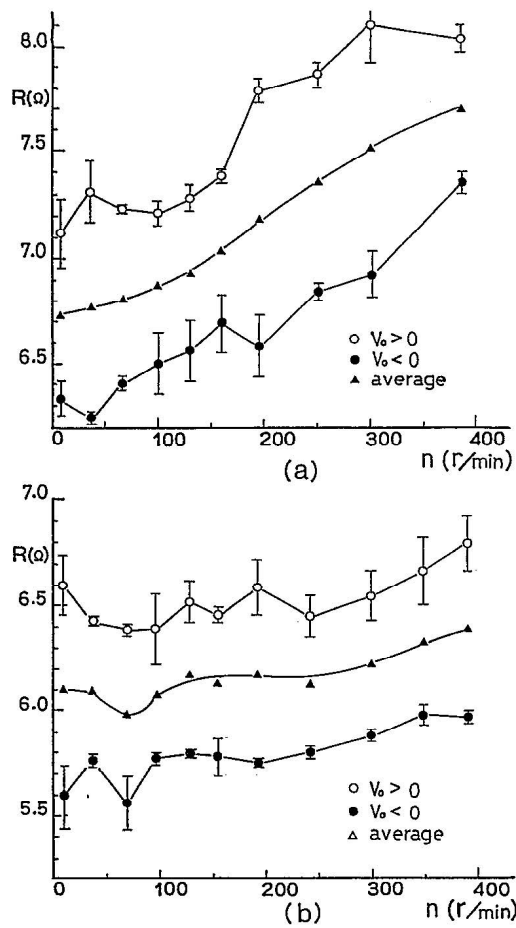
FIG. 9. Results of the experiment—apparent resistance (R) for (a) the attracting mode, and (b) the opposing mode.

$$V_1 = d(LI)/dt = d[(L_0 + \alpha v t)I]/dt$$

$$= (L_0 + \alpha v t)(dI/dt) + \alpha v I, \tag{9}$$

where v is a constant.

The terminal voltage of capacitor V_c is expressed as

$$V_c = (1/C) \int I dt, \tag{10}$$

where C is a capacitance.

By applying Kirchhoff's law to V_1, V_c, and the voltage resulting from resistance R and current I, the following equation is obtained:

$$(L_0 + \alpha v t)(dI/dt) + (1/C) \int I dt + (R + \alpha v)I = 0. \tag{11}$$

This differential equation can be solved by using the Runge–Kutta process with initial conditions $t=0$, $V=V_0$, and $I=0$.

Figure 10 and Table I show the computer simulation of the solution of this equation for the specific values of V_0, C, α, v, and R, as compared with the experimental results. The value of α is obtained from the slope of the L-d curve (Fig. 6) at L_0. The value of v is calculated from the core's rpm (revolution per minute) and the traveling distance at one rotation.
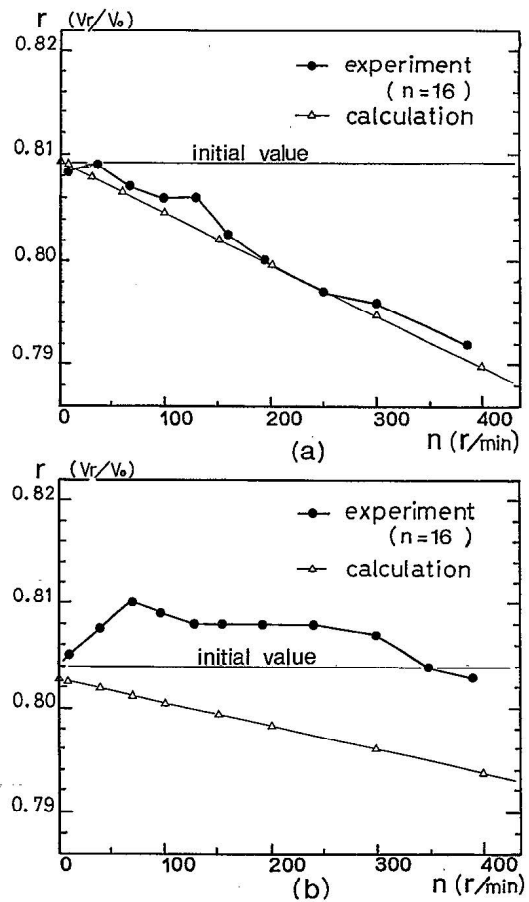
FIG. 10. The computer simulation of the Eq. (11), as compared with the experimental results: (a) the attracting mode, and (b) the opposing mode.

The simulation predicts that the recharge voltage will decrease as the core speed increases. This conforms well with the experimental results in the attracting mode. In the opposing mode, however, certain discrepancies can be found between the simulation and the actual results.

V. DISCUSSION

The mathematical analysis in the previous section reveals that the recharge voltage decreases as the core speed increases. With a constant core speed, it predicts that the recharge voltage will decrease as α increases.

The reason for the decrease in the recharge voltage can be given as follows. The displacement of the core during discharge means there is a mechanical output in the system. It is reasonable to conclude that the mechanical motion of the core is compensated for by a decrease in recharge voltage. The cause of the increase in the apparent resistance R is

TABLE I. Specific values of the simulation.

	V_0(V)	C(μF)	L_0(mH)	R(Ω)	α(H/m)	v(m/s)
Fig. 10(a) attracting mode	240	15.87	36.1	6.41	0.285	0.01665×n
Fig. 10(b) opposing mode	240	15.87	29.9	6.06	0.119	0.01665×n
						n(r/min)

57

considered to be the back EMF generated by the movement of the core. For a constant rotor speed, it is clear that a coil with a large α has a large attracting force.

However, the results differ in the case of the opposing mode. Though α is positive, r increases over the range up to a certain speed. After the peak, r decreases slightly but remains greater than the initial value.

These results can be explained from the assumption that the complex movement of the flux could generate a positive EMF: the increase in the recharge voltage is due to an EMF in the same direction as the discharge current, different from the back EMF caused by Faraday's law.

The past controversy concerning electromagnetic induction might shed some light on this viewpoint. On this topic, several authors have stated that the motional EMF caused by the cutting of the magnetic flux and the induced EMF caused by Faraday's law were independent phenomena.[4,5] These two different types of EMF are generally expressed by the following equation:

$$V = -d\Phi/dt + \int_0^l (B \times v)dl. \tag{12}$$

It can be postulated that these two types of EMF have contradicting effects within the coil, and that the motional EMF has a positive effect on the recharge voltage over a certain range of core speed.

This hypothesis seems to be consistent with the results, but is also highly speculative. It would be necessary to confirm its validity through further experimentation.

VI. CONCLUSIONS

In this paper, the behavior of an *LCR* circuit with a movable ferromagnetic core was discussed. The increase in the inductance of the coil, which is caused by the attraction of the core during discharge, yielded the following results.

(1) The recharge voltage is generally smaller when the core moves than when it is stationary. The decrease in the recharge voltage depends on the rate of change of the inductance. The simulation based on the theoretical equation confirmed the experimental results.

(2) When applying opposing magnetic fields to the facing coils, an increase in the recharge voltage can be observed in an electrically closed *LCR* circuit. The apparent resistance of the coil decreased correspondingly.

(3) It can be postulated that the complex movement of magnetic flux generates a positive EMF, but the cause of the voltage increase is not clear.

[1] J. J. Blakley, IEEE Trans. Magn. **MAG-19**, 1570 (1983).
[2] B. H. Smith, IEE **114**, 1707 (1967).
[3] S. Kikuchi, Y. Sakamoto, and K. Murakami, IEEE Trans. Magn. **MAG-20**, 1792 (1984).
[4] G. Cohn, Electrical Eng. **68**, 441 (1949).
[5] P. Moon and D. Spencer, J. Franklin Institute **260**, 213 (1955).
[6] J. C. West and B. V. Jayawant, Institution Electrical Eng. **109A**, 292 (1962).
[7] G. W. Swift, IEEE Trans. Power Apparatus Systems **PAS-88**, 42 (1989).

6020   J. Appl. Phys., Vol. 77, No. 11, 1 June 1995   Osamu Ide

58

Qualification and Quantification of Telomeric Elongation Due to Electromagnetic Resonance Exposure

Scott C Kelsey

Graduate Assistant
Department of Biomedical Sciences
Missouri State University
Kelsey6@live.missouristate.edu

Abstract. High frequency electromagnetic resonance (EMR) due to electromagnetic fields (EMFs) can directly affect intercellular molecular mechanisms. Formerly thought to have no direct impact on biological tissue an increasing amount of evidence supports that EMFs can alter the way that cells transcribe proteins, regulate cellular maintenance or enter/bypass senescence. Repeated electromagnetic field shock (REMFS) will up regulate the HSR/HSF1 pathway in young cells within mice delaying senescence directly leading to upkeep in tissue maintenance compared against control mice. In this particular case the REMFS act as an environmental stressor activating a cell signaling cascade elucidates a response within the cell that ultimately up-regulates repair and maintenance systems (Perez, 2008). One particular protein generally involved in maintenance and repair is telomerase reverse transcriptase (*h*TERT). Due to the end replication problem of semi-conservative replication of DNA each time a cell divides approximately 50-100 base pairs are lost from the ends of chromosomes. In order to prevent loss of important genetic sequence, DNA incorporates molecular "aglets" called telomeres that are simply a short hexo-nucleotide sequence of "TTAGGG" which can only be restored via *h*TERT. However, *h*TERT is only minimally active in mature mammalian cells to a continual loss of telomeric DNA in cells of adult organisms, senescence of those cells and ultimately leads to the phenomenon aging (Weaver, 2008). If aging is simply the manifestation of short telomeres then the restoration of telomeric sequence should have the reverse effect. Activation of *h*TERT in aged telomerase deficient mice indicates chromosomal telomere elongation leads to increased cellular proliferation, organ upkeep and performance and an overall physiologically "younger" appearing mouse (Jaskelioff, 2010). My colleague, Dr Norm Shealy of Holos University, has worked with EMFs as alternative medical treatment since the early seventies and has utilized several devices in his practice to treat an array of ailments from depression to cancer. One such instrument consists of an electric spark tester and a copper conductor that when current is applied emits oscillating EMFs with frequencies between 54 and 78 GHz. We speculated that this particular range of frequencies possibly acts upon either some aspect of the SUMOlynation pathway or the ubiquitin pathway associated with telomerase as human studies, performed by Dr. Shealy, indicate a consistent increase in telomere length of leukocyte DNA. In order to qualify this claim a series of primary cell lines isolated from *Mus musculus* (lab mouse) were subjected to this oscillating frequency for 30 minutes a day for approximately 4 months and telomeric regions were measured via Monochromatic Singleplex QPCR. The results appeared to indicate telomere maintenance and subtle elongation. A second set of tissue cultures are undergoing the identical treatment and will be subjected to quantification of telomere length via Southern Blot to be compared against negative controls.This will allow relatively fast assessment of the amount of telomere elongation or loss with treatment when compared to the expected loss of telomeres over a given amount of time.

Introduction

Most mammalian somatic cells will divide and eventually enter a senescent state. However, stem-cells retain their ability to divide almost perpetually due to their ability to maintain their telomeres. Telomeres are repetitive sequence that occur at the ends of chromosomes and act as molecular aglets to protect important regions of DNA. During replication a small portion of telomeric DNA is lost and when telomeres become heavily eroded the cell will enter senescence. The activation of telomerase, a telomere building protein, in somatic cells in mice leads to an increase in organ upkeep and even for cells to

revert from senescence to an actively dividing state. In addition, electromagnetic field stimulation of cell lines *in vitro* stimulates cell signaling pathways that lead to an array of transcriptional activation. If telomerase can be activated via electromagnetic resonance exposure within the cell it could lead to an increase in cellular upkeep without the administration of drugs.

Aim

To first qualify then quantify changes in telomeric length in cell lines exposed to a specific range of electromagnetic resonance between 54 and 78 GHz at 50 to 75 decibels for 30 minutes a day and compare against cell lines from the same original culture. Cell passages occur every two to three weeks at which time genomic DNA samples are taken, quantified via NanDrop and telomere length is measured with singleplex and monochromatic multiplex QPCR and southern blot analysis. Post qualification and quantification telomerase levels will be measured via RTPCR and a possible mechanism will be explored for the activation of telomerase via electromagnetic resonance exposure.

Method…

- Cell lines isolated from *Mus musculus* common lab mouse) using cold trypsinization technique
- Cell lines maintained daily and overall health assessed by visualization with phase contrast optics
- Cell lines treated with electromagnetic resonance for 30 minutes a day under sterile hood, negative control group placed under sterile hood in adjacent lab for 30 minutes a day
- Telomeric lengths assessed using the southern blot technique and singleplex and multiplex monochromatic QPCR
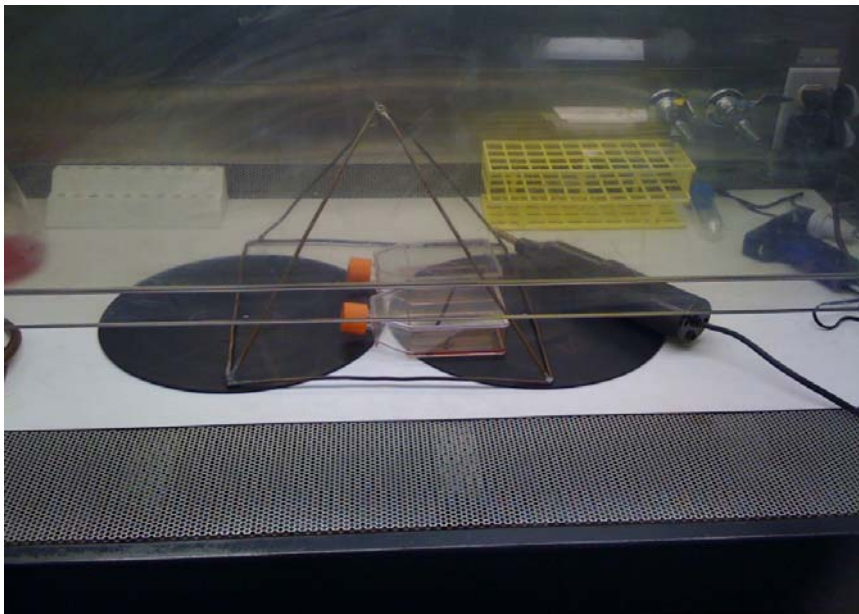
Cell cultures under tissue hood during treatment with electromagnetic resonance

Negative control cell cultures under an adjacent hood during exposure time of experimental cultures

Results

The preliminary work for this project involved treating 2 separate fibroblast cell culture isolated from either a kidney or liver of *Mus musculus.* Singleplex QPCR was used to measure relative telomere length against a single copy gene copy known to occur only one time within the mouse genome and creating a PCR product of a known size. This allows for relative calculation of telomeric repeats against the known size of the single copy gene copy PCR product.

With each cell division, due to the mechanism of DNA polymerization, between 50 and 200 nucleotides are lost from telomeric ends. Fibroblasts in cell culture will divide 2-6 times per passage depending on growth factor concentration and flask volume. Therefore, telomeric regions will experience a gradual decay of 100-1200 nucleotides per cell passage under normal circumstances.

The following graphs illustrate the relative telomere length acquisition from singleplex QPCR. The singleplex technique was performed in duplicate to ensure values remained relatively consistent. This preliminary data was performed to justify continuation of the experiment using larger sample sizes and more sensitive techniques.

The figure on the next page illustrates relative telomere length against single copy gene copy amplicon lengths at DNA isolation intervals. Under normal circumstances, a gradual decline in length would be expected due to telomere decay.

Singleplex QPCR was performed a second time to ensure that telomere decay was indeed halted by electromagnetic resonance exposure

Conclusion

The data from the preliminary experiments appears to support that electromagnetic exposure at this frequency is somehow effecting telomeric maintenance. According to the data generated from the singleplex PCR telomeric lengths are maintained and in some instances elongated. After 20-30 passages in culture telomers normally erode to a critical point that triggers cells to enter senescence. The graphs, however, show a maintenance of telomere length even into relatively old age of the cell cultures.

Unfortunately, in the original experiment negative control cell lines were placed in an adjacent sterile tissue hood within 1 meter of the treated cells. It appears that negative control group may also have been receiving treatment as there telomeres were maintained as well. The sterile tissue hoods used in this experiment are primarily composed of aluminium and stainless steel, both great conductors of electromagnetic fields. Therefore, both hoods may have been acting as large antennae amplifying the electromagnetic signals.

The Telomere
– Function and Synthesis

1. The mysterious telomere
The telomeres appear to protect the chromosomes from damage. But how?

Telomere = Greek for "end" (*telos*) and "part" (*meros*)

Cell

Chromosome

Telomere

The telomeres form caps at the ends of chromosomes. They contain a unique DNA sequence which is repeated several times.

The DNA sequence varies slightly between species. The one shown here is from *Tetrahymena*.

2. Telomere function discovered:
Telomere DNA protects the chromosomes

Chromosomes with telomeres

Tetrahymena – a single-cell organism that lives in water

Telomere DNA

Artificial minichromosomes

Yeast cell

Yeast cell

Current and Future Work

Currently, fibroblast cultures originating from mouse kidneys, endothelial cultures originating from mouse blood vessels and astrocytoma cultures originating from human

neural tissue are under investigation for the effects of electromagnetic resonance exposure on telomeric regions of DNA and will be subjected to southern blot analysis and monochromatic multiplex QPCR, both more sensitive techniques than singlex QPCR. In the future telomerase activity will be measured and ultimately a mechanism will be investigated to determine the pathway activated by electromagnetic exposure that elicits the telomeric response.

REFERENCES

Jaskelioff M, Muller FL, Paik JH, Thomas E, Jiang S, Adams AC, Sahin E, Kost-Alimova M, Protopopov A, Cadiñanos J, Horner JW, Maratos-Flier E, Depinho RA. Telomerase Reactivation reverses tissue degeneration in aged telomerase-deficient mice. 2010. *Nature*. Nov;28 (7328) 102-6.
Perez FP, Zhou X, Morisaki J, Ilie J, James T, Jurivich DA. Engineered repeated electromagnetic field shock therapy for cellular senescence and age-related diseases.2008. *Rejuvenation*. Dec;11(6):1049-57.
Weaver, Robert. 2008. Molecular Biology 4th ed. McGraw Hill, Boston MA. Pp. 708-10

iRi

wishes to thank all our sponsors who helped make this event possible:

GLOBAL GATEWAY FOUNDATION

ARCOS CIELOS FOUNDATION

iRENEW CORPORATION

ANONYMOUS DONOR

Thank You!